

Proceedings of the 4th OPU-HsH Japanese-German Symposium 2025 : An experimental learning program that merges cutting-edge technology with traditional craftsmanship

Teruaki Ito, Jens Hofschulte

Suggested citation:

Ito, Teruaki, and Jens Hofschulte, eds. 2025. "Proceedings of the 4th OPU-HsH Japanese-German Symposium 2025 : An experimental learning program that merges cutting-edge technology with traditional craftsmanship." In. Hannover: Hochschule Hannover. <https://doi.org/10.25968/opus-3527>.

Abstract

Proceedings of the OPU-HsH symposium on Industry 4.0 and Society 5.0. The symposium was held on February 14th 2025 in Okayama, Japan with members of the Okayama Prefectural University and the Hochschule Hannover. It was sponsored by the Sakura Science Program of Japan.

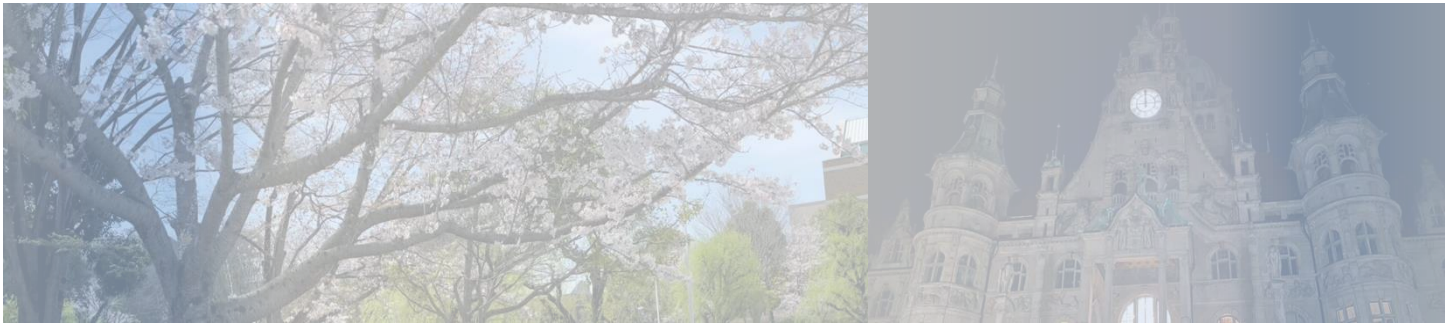
Terms of use

CC BY-ND 4.0

This document is made available under these conditions:
Creative Commons - CC BY-ND - Namensnennung - Keine Bearbeitungen 4.0 International
For more information see:
<https://creativecommons.org/licenses/by-nd/4.0/deed.de>



Proceedings of the
4th OPU-HsH Japanese-German Symposium 2025
- An experimental learning program that merges cutting-edge
technology with traditional craftsmanship -
February 14th, 2025
<https://www-ki.ss.oka-pu.ac.jp/ohjg2025/>



OHJG2025

Organized by: Okayama Prefectural University &
Hannover University of Applied Science and Arts

Sponsored by Sakura Science Program of Japan Science and Technology Agency

Edited by Teruaki ITO and Jens HOFSCHULTE

Host: Okayama Prefectural University

Organizer: Okayama Prefectural University, Japan
and Hanover University of Applied Sciences and Arts, Germany

Sponsor: Sakura Science Program by Japan Science and Technology Agency (JST)

OPU-HsH Japan-German joint committee

Akio GOFUKU (Okayama Prefectural University), Honorary Committee Member
Teruaki ITO (Okayama Prefectural University), General Chair
Akira TSUMAYA (Okayama Prefectural University), Session Chair
Naoto HARUKI (Okayama Prefectural University), Session Chair
Takashi OYAMA (Okayama Prefectural University), Logistics Chair
Yuji HAMAMOTO (Okayama Prefectural University), Publication Chair
Shinichiro OTA (Okayama Prefectural University), Student Management Chair
Yutaka ISHII (Okayama Prefectural University), VR session Chair
Masanao KOEDA (Okayama Prefectural University), VR session co-Chair
Shunsuke OTA (Okayama Prefectural University), VR session co-Chair
Tomoya YOSHIDA (Okayama Prefectural University), Venue staff
Franz KALLAGE (Hochschule Hannover - University of Applied Sciences and Arts), International Organizer
Jens HOFSCHULTE (Hochschule Hannover - University of Applied Sciences and Arts), International Organizer
Rüdiger KUTZNER (Hochschule Hannover - University of Applied Sciences and Arts), International Organizer
Viola WEDEKIND (Hochschule Hannover - University of Applied Sciences and Arts), International Organizer
Günter KLAWITTER (Hochschule Hannover - University of Applied Sciences and Arts), International Organizer
Meike MARTEN (Hochschule Hannover - University of Applied Sciences and Arts)

Invited talk:

Tetsuro OGI (Keio University)

Presenters:

Jun FURUTA (Okayama Prefectural University)
Tomoya YOSHIDA (Okayama Prefectural University)
Manato KANESAKI (Okayama Prefectural University)
Stephen Detlef HOELZEL (Hochschule Hannover - University of Applied Sciences and Arts)
Frank STOLLMEIER (Hochschule Hannover - University of Applied Sciences and Arts)
Mike OTTO (Hochschule Hannover - University of Applied Sciences and Arts)

Poster Presenters:

Jasper DEHMEL (Hochschule Hannover - University of Applied Sciences and Arts)
Christoph SCHMITT (Hochschule Hannover - University of Applied Sciences and Arts)



© 2025 Okayama Prefectural University and Hochschule Hannover
This work is licensed under a creative commons [CC BY NC 4.0](https://creativecommons.org/licenses/by-nc/4.0/) license
except images labeled with a reference source.

Contents

<i>Preface</i>	4
<i>Message from HsH for OHJG2025</i>	5
<i>Engineering a tablet filling system with codesys 3.5</i>	6
Jasper Dehmel	
<i>CFD-Based simulation and optimization of a rotary chamber machine</i>	8
Christoph Schmitt, Klaus Becker, Martin Gottschlich, Ulrich Lüdersen	
<i>Motion capture experience using mocopi</i>	13
Shunsuke OTA	
<i>Future Society by Integration of VR and AI Technologies</i>	14
Tetsuro OGI	
<i>A Storage Circuit Design for Suppressing Radiation-induced Errors in FD-SOI Processes</i>	18
Jun FURUTA, Shotaro SUGITANI, Ryuichi NAKAJIMA and Kazutoshi KOBAYASHI	
<i>A preliminary study to accurate far-localisation for wireless energy transfer in electric vehicles</i>	22
Stephen Hoelzel, Heiko Hepp	
<i>Respirometer by a piezo device and its application to triage</i>	26
Tomoya YOSHIDA	
<i>Using deep learning for plant root point detection in agricultural robotics</i>	27
Frank STOLLMEIER, Liu WANGCHU, Hanno HOMANN	
<i>Bonding of CFRTP and SPCC Using Porous Plating and Evaluation of Strength by Single-Lap Shear Test</i>	30
Manato KANESAKI*, Kazuki TSUJIKAWA**, Tadao FUKUTA and Koichi OZAKI	
<i>AI Light Room – Intelligent Lighting for Unconscious Patients in Anesthesia and Intensive Care</i>	31
Mike OTTO, Jens Christian WILL, Yavuz KÖCER	
<i>Agenda</i>	35

Preface

Teruaki ITO* & Jens HOFSCHULTE**

* Faculty of Computer Science and Systems Engineering, Okayama Prefectural University
111 Kuboki, Soja, Okayama 719-1197, Japan
E-mail: tito@ss.oka-pu.ac.jp

** Faculty I – Electrical Engineering and Information, Technology
Hochschule Hannover University Applied Science and Arts
Ricklinger Stadtweg 120, 30459 Hannover, Germany
Email: jens.hofschulte@hs-hannover.de


On behalf of the Organizing Committee of OPU-HsH Japan-Germany Symposium 2025 (OHJG2025), it is with great honor and pleasure that we welcome all of the participants to OPU-HsH Japan-Germany Symposium 2025, to be held on 14 February, 2025, at Okayama Prefectural University Campus, Okayama, Japan. We appreciate the help of the main sponsoring bodies, Sakura Science Program of Japan Science and Technology Agency (JST) as well as the co-organizing body of Okayama Prefectural University, Japan and Hochschule Hannover University Applied Science and Arts in Germany, who have made us to this symposium as a memorable and valuable event.

The first OHJG2022 was supposed to be held in OPU but shifted to virtual due to the COVID19 pandemic situation. Thanks to the continuous support from JST, Organizing Committee of OHJG2023, the second OHJG2023 was held on site where the delegates from HsH and participants from OPU had a face-to-face discussion on the various topics presented in this symposium under the title of Industry 4.0 and Society 5.0 for smart society. The third OHJG2024 welcomed Professor Umeda from the University of Tokyo to deliver a keynote address, focusing on the latest technology related to Smart Manufacturing in Japan as well as a total of six presentations from OPU and six from HsH, each covering the latest technologies being conducted at their respective universities.


In this fourth edition of the conference, we are honored to welcome Professor Ogi from Keio University to deliver a keynote address, focusing on the latest technology regarding Future Society by Integration of VR and AI Technologies. Furthermore, there will be a total of three presentations from OPU and three from HsH, two poster presentations from HsH, and three VR demonstrations by OPU, each covering the latest technologies being conducted at their respective universities.

The committee members of OHJG2025 join us in thanking every one of the presenters for their valuable contribution towards the success of this symposium, and wish all of the participants a professionally rewarding and enjoyable event.

Symposium Co-chair of OHJG2025
Okayama Prefectural University


Prof. Teruaki ITO

Symposium Co-chair of OHJG2025
Hannover University of Applied Science and Arts


Prof. Jens HOFSCHULTE

Message from HsH for OHJG2025

Franz Christoph KALLAGE*

* Faculty II – Mechanical and Bio Process Engineering
Hochschule Hannover University Applied Science and Arts
Ricklinger Stadtweg 120, 30459 Hannover, Germany
Email: franz-christoph.kallage@hs-hannover.de

When Prof. Jens Hofschulte asked me to substitute him at the OHJG2025 at Okayama Prefectural University Campus (OPU) on short notice I immediately agreed. It was my great honor and pleasure to support the symposium on-site in 2025 as representative of Hannover University of Applied Sciences and Arts (HsH). I would like to express my thanks to Sakura Science Program of JST for their sponsorship and my appreciation to Prof. Teruaki Ito and the staff of OPU for perfectly hosting the event and their warm hospitality.

I am looking forward to hearing presentations of the researchers of OPU and HsH with very fruitful discussions about VR Technology and other aspects of technology development and smart society during the symposium. I am sure that the invited speech given by Prof. Ogi, focusing on the latest technology regarding Future Society by Integration of VR and AI Technologies, will very interesting and inspiring. I think the collaboration between the Japanese and German researchers will be amazing and the conference will be a memorable event and a starting point for further collaborations.

February 2025



Prof. Franz Christoph KALLAGE

Engineering a tablet filling system with codesys 3.5

Jasper Dehmel

Faculty II – Mechanical and Bioprocess Engineering, Technology
Hochschule Hannover University Applied Science and Arts
Ricklinger Stadtweg 120, 30459 Hannover, Germany
Email: jasper.dehmel@stud.hs-hannover.de

Keywords: Codesys, Education, Simulation, PLC Programming, Sensor integration

1. Introduction

The implementation of a tablet filling system serves as an educational project within the mechanical engineering curriculum [1]. It allows students to gain hands-on experience in PLC (Programmable Logic Controller) programming and industrial automation while bridging the gap between theoretical concepts and practical applications. The objective was to develop a control system for a tablet filling station using CODESYS 3.5 [2], focusing on SFCs (Sequential Function Charts) and improving students' understanding of industrial sensors, actuators, and process control. Beginning with programming basic FBD (Function Block Diagram) circuits, which can be controlled with the buttons from the Hardware Panel (Fig. 1), students learned fundamental logic structures. Through understanding the use of the FBD compared to the SFC, students iteratively refined their automation logic and troubleshooting techniques, deepening their insight into real-world PLC applications and finally creating their own automated program.

2. System Design and Operation

The tablet filling system is designed to automate the dispensing of pills into containers through a conveyor-based system. It includes three sensors positioned at different locations along the conveyor belt to detect container positions. The middle sensor ensures that a container is accurately stopped at the filling position before activation of the pneumatic cylinder, which dispenses the predefined number of tablets (Figure 1).

The students are supposed to check the position detection of the cylinder with sensors for the ending positions. The entire operation is managed through PLC-based control, ensuring a smooth and automated sequence of steps.

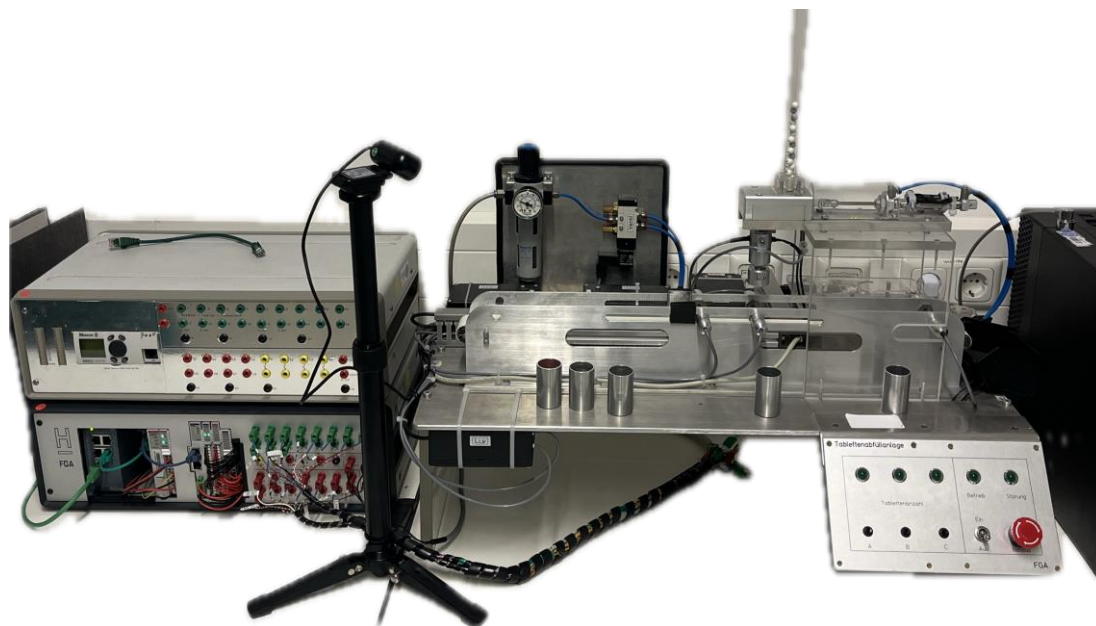


Figure 1 Tablet Filling System

An example process with one container works as follows:

- The "Process" lever is switched, and the desired number of pills to be dispensed into the container is selected.
- The conveyor belt moves the containers from left to right at high speed, if no other container is currently in the system.
- As the first sensor detects a container, the conveyor slows down to ensure smooth movement into the dispensing zone.
- Once the second sensor registers the container's presence, the conveyor stops, and pills are dispensed until the selected amount has been reached.
- The conveyor resumes operation, transporting the filled container toward the final sensor, which stops the belt until the container is retrieved.

3. Integration of Modbus and the FGA Lab Panel

A significant enhancement in CODESYS 3.5 [2] is the integration of external hardware using Modbus communication. This feature allows the connection between the PLC and external interfaces such as the FGA Lab Panel (Figure 2), a hardware panel with physical push buttons that enable manual control. The Modbus connection enables real-time data exchange, improving both troubleshooting and hardware diagnostics. This integration offers students a more realistic simulation environment, combining digital visualization with tangible hardware interaction.

4. Learning Outcomes and Challenges

The students had to face several different programming tasks which were each evaluated. After they proved that they can handle the implementation and analysis of basic function block circuits they have to write an overview of the program in form of a Process Flow Diagram. Finally they program the function of the Pill Filling System in SFC logic. Throughout the project, students developed several technical skills, including programming PLC logic, understanding sensor integration, debugging timing and synchronization issues. However, they also faced various challenges, such as working on a project as a team, debugging, and managing execution timing and synchronization in real-time system testing. Addressing these challenges helped students reinforce their problem-solving skills and gain deeper insights into automation engineering. The practical implementation of the program taught them valuable skills.



Figure 2 FGA Lab Panel[4]

5. Future Enhancements and Conclusion

From an educational standpoint, the project proves to be highly beneficial, as students reported a clearer understanding of PLC automation and control logic. The structured test phases allowed them to transition effectively from theoretical coursework to practical implementation, improving their ability to diagnose and refine automation systems. Future iterations of the project could introduce extended visualization elements to further enhance system monitoring and user interaction. Additionally, improvements in sensor calibration techniques could enhance the accuracy of the automation process.

This project successfully demonstrates the effectiveness of hands-on automation tasks in engineering education. By integrating theoretical learning with practical experience, students are able to develop critical skills in PLC programming, sensor integration, and industrial control systems. The continued expansion of such projects will further strengthen automation education, preparing students for future challenges in the field of industrial automation.

References

- [1] Hanover University of Applied Sciences and Arts. (2019). Module Handbook. HSH University of Applied Sciences and Arts Faculty II. https://f2.hs-hannover.de/fileadmin/HsH/Forms/Fakultaet_II/Modulhandbuecher/IIM-WS2019-Modulhandbuch.pdf
- [2] Codesys Group (2021). Codesys: version 3.5 SP11, <https://www.codesys.com/>
- [3] Prof. Dr.-Ing. J.Hofschulte. (2018). *Entwurf und Inbetriebnahme einer Steuerung für eine Tablettenabfüllanlage*, Hanover University of Applied Sciences and Arts Faculty II.
- [4] P. Hoffmann. (2024). *Hinweise zum Testat1 mit CODESYS3.5*. Hanover University of Applied Sciences and Arts Faculty II.

CFD-Based simulation and optimization of a rotary chamber machine

Christoph Schmitt, Klaus Becker, Martin Gottschlich, Ulrich Lüdersen

Faculty II – Mechanical Engineering and Bioprocess Engineering

Hochschule Hannover University Applied Science and Arts

Ricklinger Stadtweg 120, 30459 Hannover, Germany

Email: Christoph.schmitt@stud.hs-hannover.de

Keywords: CFD, moving meshes, Isentropic efficiency, Different intake scenarios, Thermodynamic optimization

As part of ongoing research at the Research Center Energie - Mobilität - Prozesse (FZ EMP), UAS Hannover, the following machine, referred to as a rotary chamber machine, has been further developed and adapted for demanding industrial applications. A compact version of this machine was designed, built, and tested at a laboratory scale under real conditions. The rotary chamber machine is considered in this study as a compressor system, performing the compression step required in various thermodynamic processes.

The rotary chamber machine is based on two intermeshing rotors, each with four blades, which perform a phase-shifted motion relative to each other by means of special toothed or eccentric gears (see Figure 1). Both rotors rotate in the same direction and are driven by a common main shaft. While one rotor accelerates, the other rotor decelerates and vice versa. This results in volume pulsation between the vanes, which form the working chambers of the machine where the suction and compression of the working fluid takes place.

The changing angular velocities of the rotors and the working chambers are shown over one main shaft revolution in Figure 2. A total of 32 working cycles take place in one main shaft revolution. These ensure a high volume throughput. The machine continues to operate oil-free and without valve mechanisms according to the slide-valve principle and is thus characterized by low-maintenance operation over the long term.

The operational requirements and optimization potentials of the machine are supported by numerical calculations and simulations with a commercial CFD solver (Computational Fluid Dynamics) in order to obtain more detailed knowledge of the physical phenomena taking place and to optimize the machine according to its key performance indicators.

For the calculation of the highly transient flow behaviour occurring in the machine, high spatial and temporal resolutions are necessary. In addition, the description of the pulsating working chambers according to the function in Figure 2 which are described by moving meshes, is required. The distortions of the moving meshes cause a difficult convergence behaviour, which makes a high resolution indispensable for the compliance with the topology. Therefore, meaningful parameter studies can only be computed on clusters (NHR@Berlin) due to the high computational capacity required [1].

The internal isentropic efficiency, which neglects the mechanical power component of the coupling power, is used

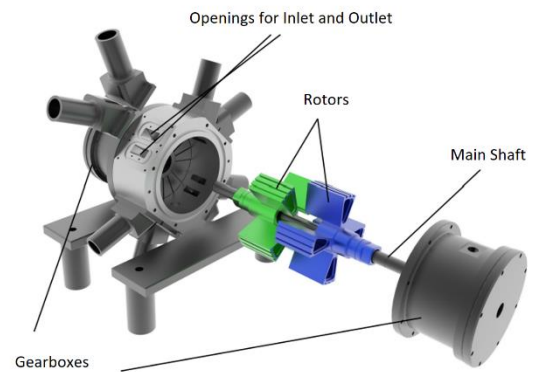


Figure 1: Structure of the rotary chamber machine with its main components.

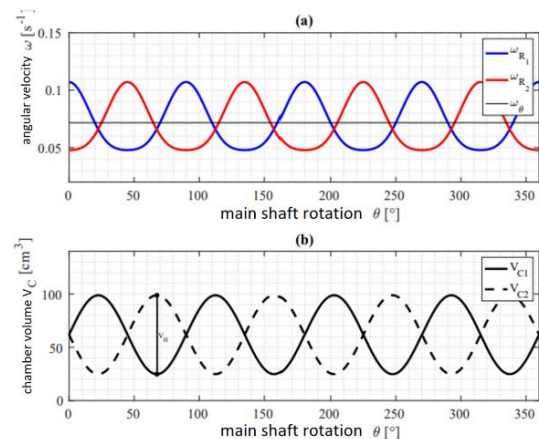


Figure 2: (a) Angular velocities of rotors ω_{R1} , ω_{R2} and main shaft, $\omega_N = \text{const.}$, (b) chamber volume profile V_C during one main shaft revolution.

to determine efficiency. It is defined in equation (1) as follows:

$$\eta_{i,is} = \frac{P_{is}}{P_i} = \frac{\dot{V}_1 \cdot p_1 \cdot \frac{\kappa}{\kappa - 1} \cdot \left[\left(\frac{p_2}{p_1} \right)^{\frac{\kappa - 1}{\kappa}} - 1 \right]}{P_i} \quad (1)$$

Here, P_i is the internal power, and the numerator represents the isentropic power. The internal power is determined from the contour integral of the p-V-diagram (internal work) as well as the rotational speed (equations (2) and (3)) [2].

$$P_i = W_i \cdot n \quad (2)$$

$$W_i = \oint V dp \quad (3)$$

In previous works [2], [3] extensive CFD parameter studies have been successfully implemented using the computational capabilities of NHR. More than 100 design points with a computing time of 11 hours each were computed in parallel on several nodes in a few days.

A PhD thesis [4] prepared as part of the research provided data on efficient operating parameters, key performance indicators and the main optimization variables. The study showed that the delivery efficiency of the present prototype is strongly speed dependent, with a local maximum of 86.8% at a speed of 1200 rpm. The numerical investigations also show that increasing the blade widths and thus reducing the dead space has a positive effect on the above-mentioned key parameters.

To achieve higher efficiencies and fluidic optimizations within the inlet and outlet ducts, further development of the machine is necessary. Further investigation focuses on the extent to which axial intake improves the machine's performance. In Figure 3 are the different geometries displayed. Variants (a) and (b) represent the axial intake, while variant (c) illustrates the current radial intake design. The blue arrows indicate the inlets, while the orange ones represent the outlets. Additionally, the comparison is made between the ideal process without leakage losses and the real process with such losses.

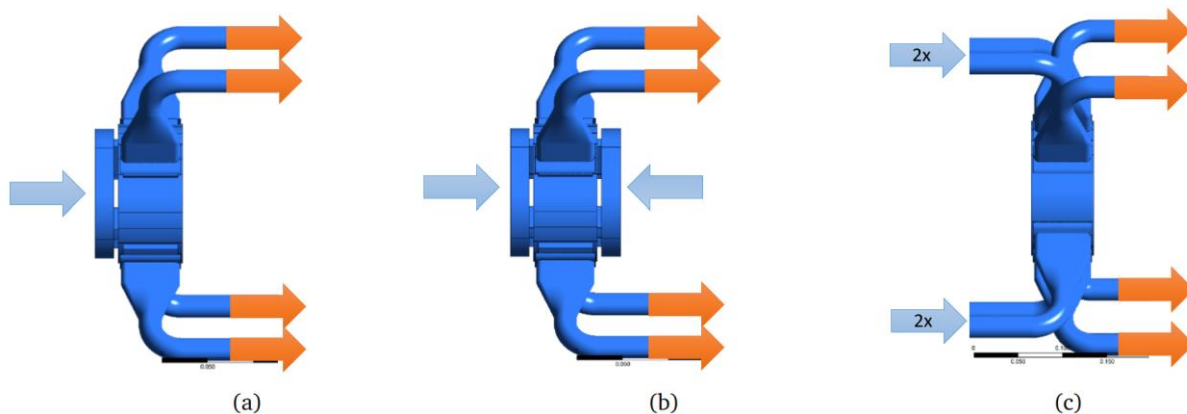


Figure 3: (a) Axial, single-side intake, (b) Axial, double-side intake, (c) Radial intake

An image of the simulation results of the machine is shown in Figure 4. In this figure, the velocity vectors during the discharge and intake processes of the working cycle with and without losses can be observed. Larger vortices form during the intake process in (b), while the discharge process exhibits high velocities. It can also be seen that leakage flow occurs through the clearance gap, allowing fluid to flow from the high-pressure chamber to the low-pressure chamber.

In (a), higher velocities occur in both cases since there are no leakage flows. The vortices in the intake process are

not as dominant as in case (b), as there are no overflow effects generating them.

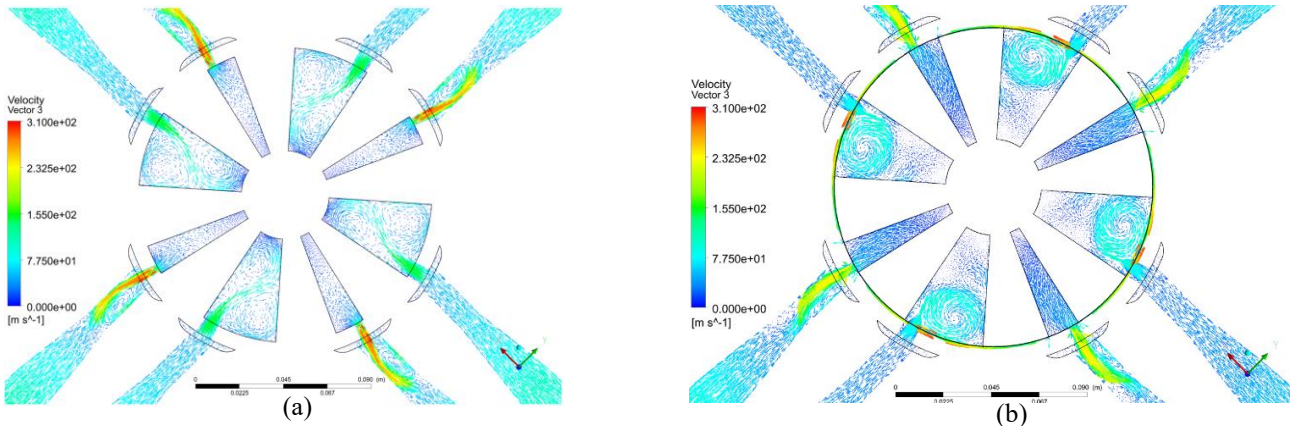


Figure 4: Simulated velocity distribution during the inlet and outlet process in the working chambers with ideal geometry (a) and real geometry (b)

Figure 5 shows the calculated results for the isentropic efficiency. It can be seen that the ideal processes, such as (a,id), clearly outperform the real processes. In all cases, single-sided axial intake is inferior to double-sided axial intake. The double-sided axial intake performs similarly to the radial intake. The radial intake proves to be the most efficient for both the ideal and real processes.

However, it should be noted that the leakage gap in axial intakes occurs not only radially but also axially and has been taken into account. These gaps increase the leakage flow of the fluid, thereby impacting the isentropic efficiency.

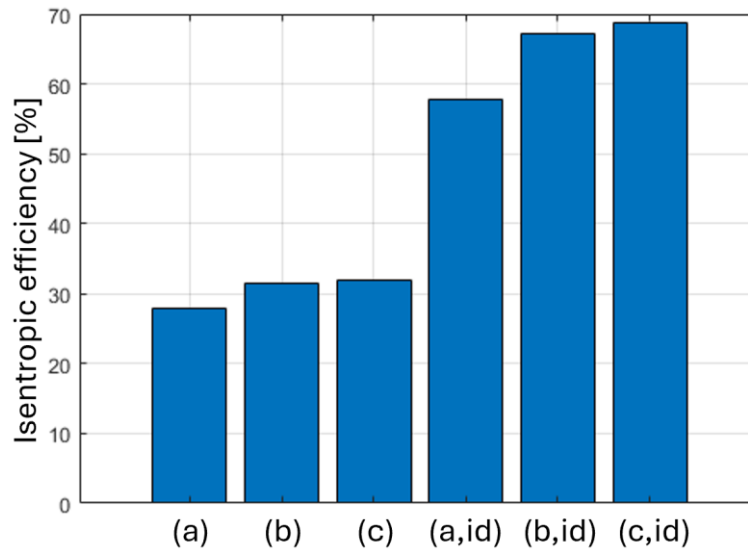


Figure 5: Isentropic efficiencies for geometrys a,b and c and without frictional or flow losses (id)

Furthermore, it must be determined whether a more compact design (axial intake) should be pursued at the expense of efficiency. Additionally, the geometry of the axial intake needs to be tested on the compressor test bench to validate the results of the CFD analysis. The sealing system requires further investigation to optimize its performance and integration with the axial intake design, gaps and velocities are shown in Figure 6.

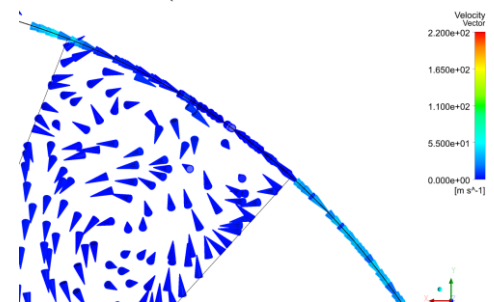


Figure 6: Leakage gaps with velocity vectors

References

- [1] Schütte. (2025). *NHR-Verein*. Berlin. Retrieved from <https://www.nhr-verein.de/>
- [2] Cui. (2021). *Parametric studies on a new Schukey type rotary compressor*. 25th International Compressor Engineering Conference at Purdue.
- [3] Schmitt, Becker, Gottschlich, & Lüdersen. (2024). *Development and optimization of a rotary chamber compressor*. Annual Meeting of Process Engineering and Materials Technology, Poster 23.
- [4] Cui. (2022). *Experimentelle und numerische Analyse eines Rotationskammer (RC)-Verdichters zur Anwendung im Lufikälteprozess*. Hannover: TEWISS. ISBN: 978-3-95900-756-6

CFD-Based Simulation and Optimization of a Rotary Chamber Machine

Christoph Schmitt*, Klaus Becker, Martin Gottschlich, Ulrich Lüdersen
Hochschule Hannover, Research Center EMP, Ricklinger Stadtweg 120, 30459 Hannover

Introduction

Technological Advantages

The Rotary Chamber Compressor (RC compressor) offers the following advantages over traditional reciprocating machines:

- No valves, only rotating components → less wear
- Higher volumetric throughput
- Better part-load behavior

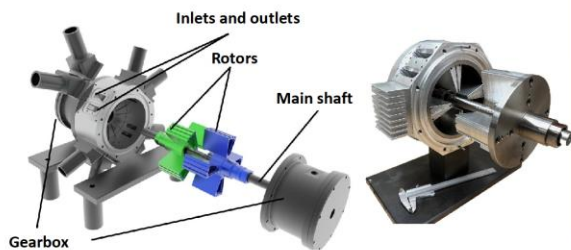


Fig. 1: Structure of the rotary chamber machine with its main components.

Simulations

Investigation focuses on the extent to which axial intake improves the machine's performance

- Simulation of different geometries for various intake scenarios with and without considering losses at the NHR@zib (HPC-Cluster) in Berlin
- (a): Axial, single-sided intake
- (b): Axial, double-sided intake
- (c): Radial intake

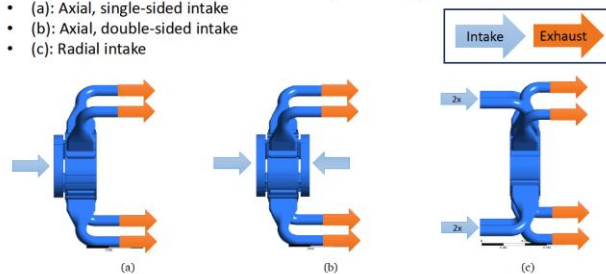


Fig. 2: Different machine geometries for various intake scenarios.

Results

Figure 3 shows the simulated velocity distribution during the intake and exhaust process for the radial intake scenario without losses (a) and with losses (b).

The increased velocities during the exhaust phase, as well as the formation of vortices during the discharge process, are clearly visible.

- The ideal geometry shows higher velocities during the discharge phase. This is because no losses are generated in the leakage gaps.
- The real geometry, on the other hand, shows lower velocities overall. High velocities can be observed in the leakage gaps, where the fluid flows along these gaps at high speed.
- The axial intakes show a similar pattern, where the fluid enters from the sides, creating vortices in the center of the chamber.

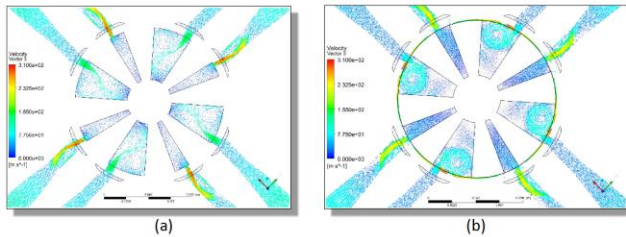


Fig. 3: Simulated velocity distribution during the inlet and outlet process in the working chambers with ideal geometry (a) and real geometry (b)

Figure 4 illustrates the calculated results for the isentropic efficiency. It can be seen that the ideal processes, such as (a,id), clearly outperform the real processes.

- Single-sided axial intake is inferior to double-sided axial intake. The double-sided axial intake performs similarly to the radial intake.
- The radial intake proves to be the most efficient for both the ideal and real processes.

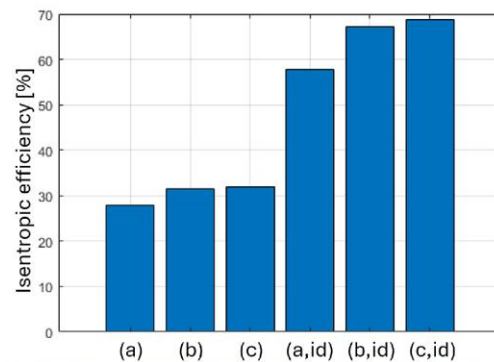


Fig. 4: Isentropic efficiencies for geometries a, b and c and without frictional or flow losses (id)

Conclusion and further work

Performance: The investigation showed that the double-sided axial intake performs similarly to the radial intake. Despite slightly lower isentropic efficiency, the space savings of the axial intake warrant further evaluation to determine if they offset the efficiency losses, impacting overall machine effectiveness.

Validation: A physical model needs to be constructed to validate the results and assess the real-world performance of the axial intake design. This also enables the determination of actual losses in the axial design.

Sealing: The sealing system requires further investigation to optimize its performance and integration with the axial intake design.

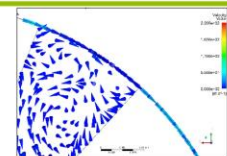


Fig. 5: Leakage gaps with velocity vectors



Contact
Christoph Schmitt
クリストフ・シュミット
christoph.schmitt@stud.hs-hannover.de

Funded by:



 Niedersächsisches Ministerium
für Wissenschaft und Kultur

 VolkswagenStiftung

Motion capture experience using mocopi

Shunsuke OTA*

* Faculty of Computer Science and Systems Engineering, Okayama Prefectural University
111 Kuboki, Soja, Okayama 719-1197, Japan
E-mail: s_ota@ss.oka-pu.ac.jp

Keywords: Motion capture, mocopi, inertial sensor

In recently years, Sony has introduced mocopi [1], a compact and affordable motion capture device designed to provide advanced motion tracking capabilities across a variety of applications (Fig. 1). Using inertial sensors, which combine accelerometers and gyroscopes, mocopi accurately captures human movement in real-time, supporting avatar video creation, motion data recording, and real-time avatar manipulation in services such as VRChat. Leveraging Sony's proprietary algorithms, mocopi achieves high-precision tracking with a minimal number of sensors, making motion capture more accessible for VTubers, filmmakers, and animators, without being constrained by time or location.

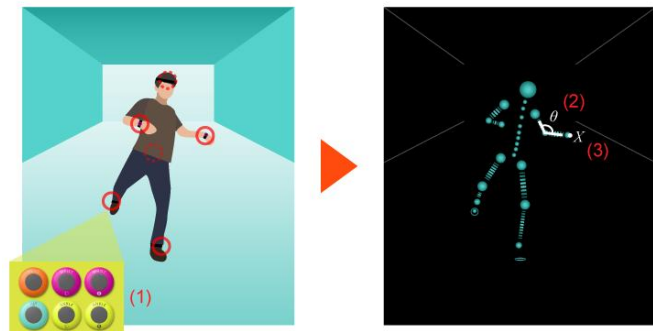


Fig. 1. Mocopi System Overview

Mocopi wirelessly connects to smartphones via Bluetooth and facilitates motion capture using a dedicated application. Each sensor measures 32mm in diameter, 11.6mm thick, and weighs only 8 grams, making it comfortable to use for long periods of time. The sensors can be easily attached with the included Velcro straps or clips, and the system is completely wireless, so no external power or cables are required, allowing for greater freedom of movement.

In November 2024, Sony launched the "mocopi VR [2]" application, allowing mocopi to function as a virtual tracker for SteamVR, enabling full-body tracking for a more immersive VR experience. Standard VR systems typically track head and hand movements using built-in sensors in head-mounted displays (HMDs) and controllers. However, full-body tracking requires additional sensors for lower body movements. To address this, Sony introduced a VR mode that enhances the accuracy of tracking for walking, running, and jumping. In this mode, mocopi sensors are worn on the waist, knees, and ankles, complementing traditional VR tracking methods and ensuring a more realistic virtual experience (Fig. 2).

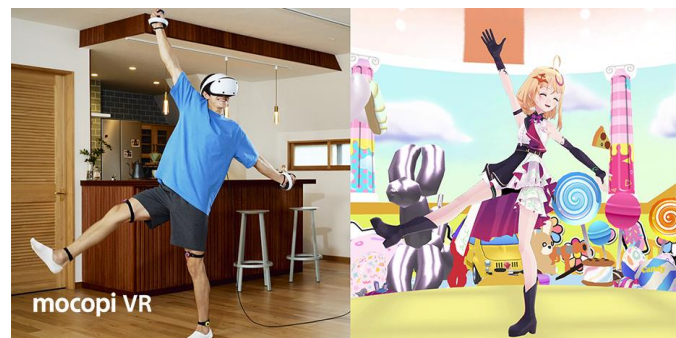


Fig. 2. Scenes of using mocopi VR

At this symposium, the mocopi experience event will provide an opportunity to experience motion tracking using mocopi. Participants will experience how improvements in motion tracking can enhance virtual interactions and explore new possibilities for human-computer interaction.

References

- [1] mocopi, <https://www.sony.net/Products/mocopi-dev/en/>
[2] mocopi VR, https://www.sony.net/Products/mocopi-dev/en/downloads/Download_mocopiVR.html

Future Society by Integration of VR and AI Technologies

Tetsuro OGI*

* Graduate School of System Design and Management, Keio University
4-1-1 Hiyoshi, Kohoku-ku, Yokohama 223-8526, Japan
E-mail: ogi@sdm.keio.ac.jp

Keywords: Virtual Reality, Augmented Reality, Artificial Intelligence, Machine Learning

Introduction

In general, research on science technology experiences booms every few decades, driven by the development of related technologies and changes in social background. In recent years, VR and AR technologies have become widely used, based on the spread of smartphones and the development of graphics board technology. AI technology has also been attracting a great deal of attention worldwide in recent years, based on the spread of the Internet and the development of GPU calculations. As a result, both VR and AI technologies have made great advances today, and it is expected that the fusion of two technologies will bring even greater changes in society. In this paper, we will discuss the future society that will be brought by the fusion of VR/AR and AI technologies while introducing our recent researches.

Deep Learning and VR/AR Technology

When experiencing a VR/AR world, the user perceives the world, processes some information in his or her brain, and takes action in the world. On the other hand, the virtual world also senses the user's action, processes some information in the computer, and presents the world. AI can substitute for or assist with both the information processing based on the user's perception and based on the sensor in the virtual world. Deep learning in the AI processing corresponds to the function of recognition and classification based on perception and sensing. Therefore, when deep learning is integrated with VR/AR systems, applications such as AI performing advanced information processing as an expert on behalf of the user, or the virtual world recognizing the user's actions and performing advanced simulations are considered as shown in Figure 1.

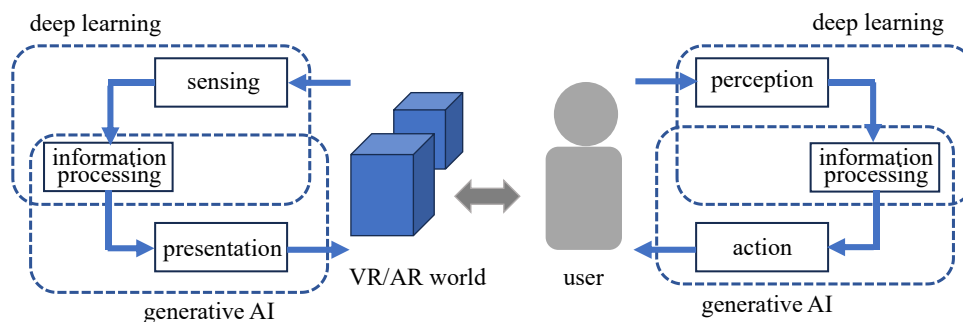


Figure 1. Integration of VR/AR and AI technologies

Figure 2 shows the AR zoo information presentation system based on deep learning developed in our laboratory. In this system, when a user directs the smartphone camera to an unknown animal in the zoo, the captured image is sent to a server in which machine learning has been performed beforehand, the animal is identified using deep learning, and explanation information about the animal is sent back to the user's smartphone and it is displayed in AR. In this case, an AI expert recognizes the animal on behalf of the user to support him or her. When building an actual system, though machine learning on animal images must be conducted beforehand, the learning needs to be updated constantly, because animals take various postures and grow over time. Therefore, when it is used at the zoo, it was linked to a new-animal exploration game app, so that if the system cannot identify the animal, user sends the image of it to the server to earn

points, and the machine learning is updated using the effect of gamification.



Figure 2. AR zoo information presentation system

Next, Figure 3 shows an experiential information retrieval system that was built by extending the deep learning based object identification function. Usually, when we see something unfamiliar, we search for information on the Internet by using its characteristics as keywords. In this system, when we see an unfamiliar object, we put on AR glasses and gaze at it. Then, an image is captured and it is identified based on deep learning. After that, a virtual world that explains the object is searched for and it is displayed as VR information. For example, when we see an unfamiliar car, we gaze at it and are transported to a virtual showroom of the car, which allows us to understand the car through the experience. The virtual world presented in this system is built as a 360-degree video using WebVR. Therefore, the virtual world information can be stored as Web information, making it possible to develop a VR information retrieval system as an extension of conventional Web searches.



Figure 3. Experiential information retrieval system

Generative AI and VR/AR Technology

In AI technologies, generative AI has been developing rapidly in recent years. The target of generative AI has expanded from text generation represented by ChatGPT, to image generation such as Stable Diffusion, and even video generation. Since generative AI can substitute the actions based on human information processing, or the presentation of the world based on information processing in the computer, when it is combined with VR/AR systems, it is possible to substitute or support the entire user's actions or the changes in the virtual world itself.

Figure 4 shows the National Diet experience metaverse system, which was constructed as an application of generative AI and VR. In Japan, the low interest of young people in politics has become a social problem. The reasons for this include the difficulty of political terminology, lack of familiarity with politicians, and lack of personal connection to the world of politics. To solve these problems, this system constructs a virtual world of the National Diet as a metaverse, expresses politicians as familiar avatars, and translates the politicians' responses into words that even children can understand through ChatGPT to have the avatars speak them. By immersing themselves in the metaverse world of the National Diet using an HMD, users can not only see and hear the National Diet, but also experience the National Diet as a personal experience by being in the same place. This system aims at promoting young people's interest and understand

of politics by combining generative AI technology with the metaverse.



Figure 4. National Diet experience metaverse system

Next, Figure 5 shows an AI facilitator avatar. A facilitator is a person who facilitates discussions in meetings and workshops, and it is required to create an environment where participants can freely speak and exchange opinions. The current conversation function of ChatGPT includes functions to support facilitation, such as requesting speech, asking questions, and summarizing opinions, etc. On the other hand, in the meetings using the metaverse space, it is known that the design of the virtual space and the expression of the avatar affects the activation of discussions. Therefore, in this study, an AI facilitator avatar was generated by integrating the facilitation function of ChatGPT into an avatar represented in the metaverse. By using this system, we conducted an experiment in which a group of some people made decisions based on discussion, and it was shown that the AI facilitator plays the same role as a human facilitator and is used effectively.



Figure 5. AI facilitator avatar.

Conclusions

This paper described the current situation of VR and AI technologies going towards fusion while introducing some examples of our research on the fusion of VR/AR and AI technologies. The integrations of VR/AR and AI technologies include applications where AI technology uses VR/AR worlds to substitute or support human activities, and applications where VR/AR worlds themselves are enhanced by AI technology. Especially, generative AI technology is evolving from images to video and even 3D model generation. In the future, virtual worlds themselves will be automatically generated by expressions using language, and AI avatars that are fully automated will also appear in the virtual worlds. Since VR/AR technology is related to all human activities, it is expected that by integrating it with AI technology, advanced virtual worlds will be constructed more easily, and new services using virtual spaces will be provided.

References

- [1] T. Ogi, Y. Takesue, and S. Lukosch, "Development of AR Information System based on Deep Learning and Gamification," The 21st International Conference on Network-Based Information Systems (NBIS 2018), 2018, pp.485-493.
- [2] X. Gao and T. Ogi, "Development of Visual Image Recognition Based VR Information Search System," The 23rd Annual Conference of the Virtual Reality Society of Japan, 2018.

- [3] K. Iwanami, H. Muto, and T. Ogi, "In-metaverse Representation of Parliamentary Broadcasts Using Avatar and AI," The 29th Annual Conference of the Virtual Reality Society of Japan, 2024.
- [4] M. Epis, and T. Ogi, "Analysis of Customized Avatars, Environments, and AI Support on Group Decision-Making in Virtual World," The 29th Annual Conference of the Virtual Reality Society of Japan, 2024.

A Storage Circuit Design for Suppressing Radiation-induced Errors in FD-SOI Processes

Jun FURUTA*, Shotaro SUGITANI**, Ryuichi NAKAJIMA** and Kazutoshi KOBAYASHI**

* Faculty of Computer Science and Systems Engineering, Okayama Prefectural University

111 Kuboki, Soja, Okayama 719-1197, Japan

E-mail: furuta@c.oka-pu.ac.jp

**Department of Electronics, Kyoto Institute of Technology

Matsugasaki Sakyo-ku, 606-8585, Kyoto, Japan

Keywords: Integrated Circuit, Circuit Reliability, Soft Error

1. Introduction

Single event effects are one of the significant issues for circuit reliability since they transiently flip the output of transistor, resulting in circuit malfunction. This malfunction is called soft error. Single event effects are caused by a charged particle. A charged particle generates electron-hole pairs in semiconductors along its track and the generated electrons are collected to the diffusion region of off-state nMOSFET by the electric field in the depletion layer as shown in Fig. 1. Thereby, the output of the off-state nMOSFET is flipped transiently. When a charged particle passes through a logic circuit, its output is inverted for a time depending on the amount of collected charge, which is called single event transient (SET). When a charged particle passes through a storage element, its stored data can be flipped by collected charge, which is called single event upset (SEU).

Fully-depleted silicon on insulator (FD-SOI) process is one of the most effective solutions to reduce single event effects. It is because a buried oxide layer can block transistors from collecting charge generated by a radiation strike without any performance overhead. However, the amount of improvement in error tolerance is still 10 – 100 times compared to bulk processes [1-3]. Some countermeasures on circuit structures are required to achieve error tolerance that can be used in a space environment. However, completely-redundant circuits such as a triple modular redundant flip-flop are excessive for FD-SOI technology [4].

Transistor stacking is a radiation-hardened methodology for FD-SOI processes [5, 6]. In FDSOI processes, single event upsets were caused by the parasitic bipolar effect which temporarily conducts between the drain and source regions of a MOSFET. Therefore, the conduction due to parasitic bipolar effects can be prevented by replacing a single MOSFET with two cascaded MOSFETs (stacked MOSFETs). Compared with redundant circuits, the transistor stacking methodology has less area penalty. However, it has large delay overhead. A radiation-hardened circuit with small area and delay penalties is required.

In this paper, we propose a radiation-hardened FF combined with a transient-fault tolerant (TFT) structure for FD-SOI technology [7]. The proposed TFT FF, standard FF and conventional stacked FFs were fabricated in a 65 nm process to compare the cross sections of single event upsets by heavy ion irradiation. Experimental tests were performed using Ar and Xe ions with linear energy transfer (LET) values of 16 MeV-cm²/mg and 69 MeV-cm²/mg, respectively.

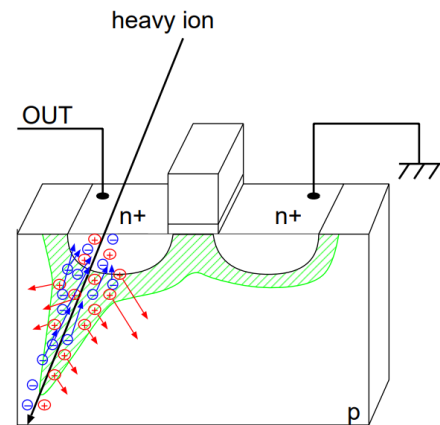


Fig. 1 Single event effect in a semiconductor device

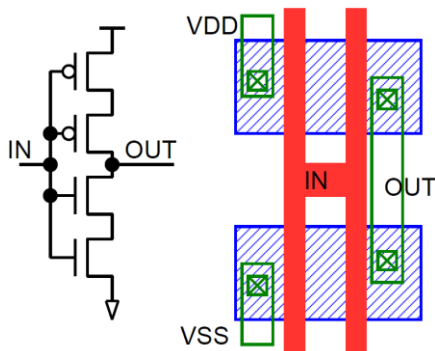


Fig. 2 Stacked inverter [5]

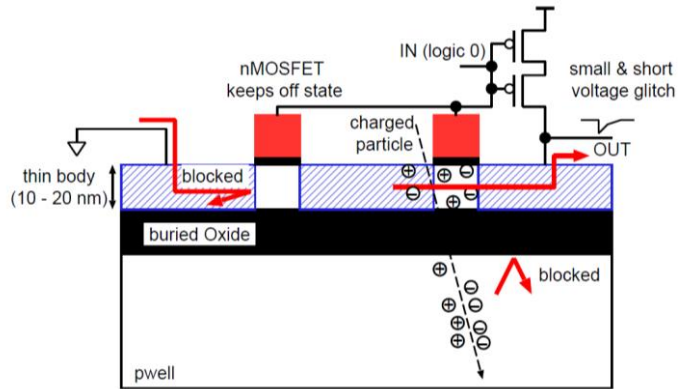


Fig. 3 Mitigation mechanism of the stacked structure.

2. Radiation Hardened Structures Suitable for FD-SOI Processes

Makihara et al. proposed the stacked inverter (Fig. 2) to mitigate a single event effectively in any SOI process [5]. When one of off-state MOSFETs is struck by a charged particle, small amount of charge is collected to the output node because the buried oxide layer blocks charge collection from substrate. Additionally, the current by the bipolar effect completely blocked by the other off-state MOSFET as shown in Fig. 3. The stacked inverter is immune to single event transients (SETs). The advantage is that there is no additional metal wiring and logic gates can be easily converted to a stacked structure with small area penalty. One of the drawbacks is the large delay penalty. Stacked logic gates have approximately four times long propagation delay time of the unstacked logic gate since their input capacitance and output resistance are doubled.

Omana et al. proposed a radiation-hardened latch for a bulk process as shown in Fig. 4 called TFT latch [8]. The feedback loop of the TFT latch consists of duplicated inverters and the C-element. Thus, an SET pulse from the inverters is blocked by the C-element. In contrast, the output of the C-element is easily flipped by a radiation strike in a bulk process. However, we find that the C-element can be considered as a stacked inverter when two input values are same, and it is immune to SETs in a FD-SOI process. As a result, the TFT latch in a FD-SOI process achieves high SEU tolerance equivalent to the stacked structure. The TFT latch has better delay performance than stacked latch structure because the duplicated inverters do not influence delay time.

We fabricated test chips in a 65nm FD-SOI process. The test chips include three kinds of FFs: a standard FF, a stacked FF and the TFT FF. All FFs construct a shift register to write and read their stored values. Table I shows the normalized circuit performance obtained from post layout simulations. Transistor sizes of each FF are optimized by the downhill simplex method to minimize the energy-delay (ED) product. The ED product of the TFT FF is half of that of the stacked FF because the delay overhead of the TFT FF is 22% of that of the stacked FF. The TFT structure was able to suppress the increase in gate capacitance as well as on-resistance and achieves better ED product than the stacked FF.

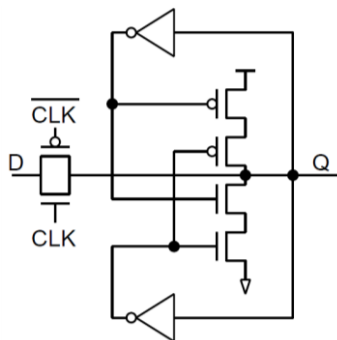


Fig. 4 Schematic diagram of transient fault-tolerant latch [8]

Table I
Performance of implemented FFs in the FD-SOI process
normalized by the standard FF

	Area	Setup time + CQ delay		Power	ED product
		rise	fall		
Standard FF	1	1	1	1	1
Stacked FF	1.22	1.68	1.65	1.04	2.89
TFT FF	1.35	1.15	1.14	1.09	1.43

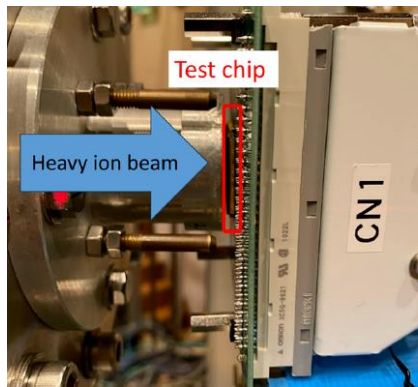


Fig. 5 Experimental setup at CYRIC

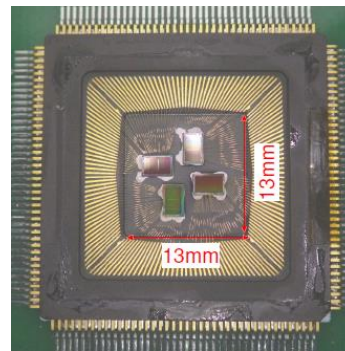


Fig. 6 Four chips in a package to increase measurement results

3. Heavy Ion Irradiation Test Results

Heavy ion experiments were performed at Cyclotron and Radioisotope Center (CYRIC) and Takasaki Ion Accelerators for Advanced Radiation Application (TIARA). We used vertically-incident $^{40}\text{Ar}^{8+}$ and $^{129}\text{Xe}^{25+}$ ions. As shown in Fig. 5, Ar ion tests at CYRIC were conducted in air and the distance between irradiation port and the test chip is about 2 mm. Therefore, energy and LET of Ar ions can be slightly reduced by air. In contrast, Xe ion tests at TIARA were conducted in a vacuum chamber. In both Ar and Xe ions irradiation tests, four chips in a package (Fig. 6) were used as a measurement target to increase the number of SEU events, which is small enough for the beam diameter because the chip size is $2.0 \times 3.0 \text{ mm}^2$. All heavy ion tests were performed in static test conditions. All FFs stored same logic values (All0 or All1) and the supply voltage was set to the nominal voltage of 1.2 V. Heavy ions were irradiated for 30 seconds, and all stored values were read out after irradiation.

Fig. 7 shows the cross sections of the FFs by Ar ions for each condition of stored values (Q) and the clock signal (CLK). The error bars in Fig. 7 represent 95% confidence intervals. The results indicate that the Ar-induced SEU rate of the TFT FF is more than three orders of magnitude lower than that of the standard FF in the 65 nm FD-SOI process. The total number of observed SEUs in the TFT FFs is 15. These SEUs are caused by charge sharing between the duplicated inverters and between the series-connected MOSFETs in the C-element [9]. To improve soft error tolerance of the TFT FF, these critical node pairs should be placed apart as well as redundant FFs in a bulk process. Fig. 8 shows the cross sections of the FFs by Xe ions. Compared with Ar ion results, the cross section of the TFT FF increased by about two orders of magnitude at (Q, CLK) = (0, 1). However, the average cross section of the TFT FF is 1/100 of that of the standard FF and the TFT FF achieved sufficient improvement of radiation resistance up to $69 \text{ MeV}\cdot\text{cm}^2/\text{mg}$.

The stacked FF achieves higher SEU tolerance than the TFT FF. It is due to the large input capacitance of the stacked structure, which increases the feedback loop delay and critical charge of the stacked FF. Since the delay overhead of the

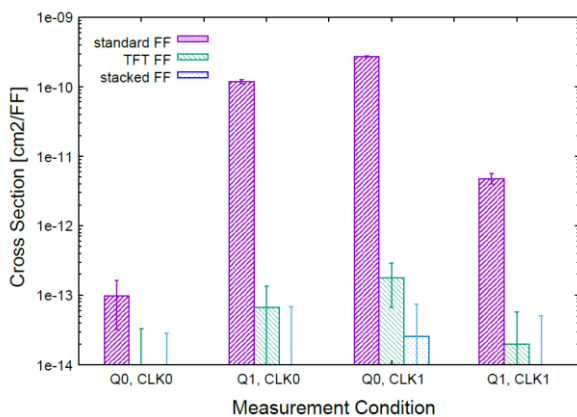


Fig. 7 Ar-ion-induced SEU rates on the 65 nm FD-SOI process

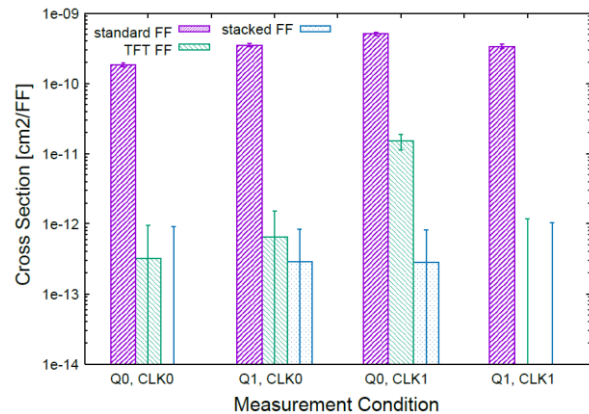


Fig. 8 Xe-ion-induced SEU rates on the 65 nm FD-SOI process

TFT FF is 22% of that of the stacked FF, the TFT FF is more effective if it is connected to critical path. In contrast, the stacked FF can provide better area efficiency and circuit reliability if it is connected to a smaller number of logic gates than the critical path.

4. Conclusion

In this paper, we report cross sections of a radiation-hardened FF combined with the TFT structure and FD-SOI technology. Experimental tests using Ar ions with LET of 16 MeV-cm²/mg show that the TFT FF achieves over 1,000x higher radiation hardness than the standard FF in a 65 nm FD-SOI process with 35%, 15% and 9% increases in area, delay time and power consumption, respectively. Although the TFT FF could not achieve equivalent radiation tolerance of the conventional stacked FF, it can achieve smaller performance overhead while achieving sufficiently high radiation tolerance since the delay overhead of the TFT FF is 22% of that of the stacked FF. To improve the soft error tolerance, each critical node pair of the TFT FF should be placed apart as well as redundant FFs, and diffusion regions of the duplicated inverters should not be shared.

Acknowledgments

The authors would like to thank Cyclotron and Radioisotope Center (CYRIC), Tohoku University and Advanced Radiation Application (TIARA) for heavy ion experiments. This work was supported through the activities of VDEC, The University of Tokyo, in collaboration with Cadence Design Systems, NIHON SYNOPSIS G.K. and Siemens Electronic Design Automation Japan K.K..

References

- [1] Philippe Roche, Jean-Luc Autran, Gilles Gasiot, and Daniela Munteanu, "Technology downscaling worsening radiation effects in bulk: SOI to the rescue," in 2013 IEEE International Electron Devices Meeting, 2013, pp. 31.1.1–31.1.4. J. Clerk Maxwell, *A Treatise on Electricity and Magnetism*, 3rd ed., vol. 2. Oxford: Clarendon, 1892, pp.68–73.
- [2] K. Kobayashi, K. Kubota, M. Masuda, Y. Manzawa, J. Furuta, S. Kanda, and H. Onodera, "A low-power and area-efficient radiationhard redundant flip-flop, DICE ACFF, in a 65 nm thin-BOX FD-SOI," *IEEE Transactions on Nuclear Science*, vol. 61, no. 4, pp. 1881–1888, 2014.
- [3] Taiki Uemura, Byungjin Chung, Jeongmin Jo, Hai Jiang, Yongsung Ji, Tae-Young Jeong, Rakesh Ranjan, Youngin Park, Kiil Hong, Seungbae Lee, Hwasung Rhee, Sangwoo Pae, Euncheol Lee, Jaehee Choi, Shota Ohnishi, and Ken Machida, "Investigating of SER in 28 nm FDSOIplanar and comparing with SER in bulk-FinFET," in 2020 IEEE International Reliability Physics Symposium (IRPS), 2020, pp. 1–5.
- [4] J. S. Kaupilla, T. D. Loveless, R. C. Quinn, J. A. Maharrey, M. L. Alles, M. W. McCurdy, R. A. Reed, B. L. Bhuvu, L. W. Massengill, and K. Lilja, "Utilizing device stacking for area efficient hardened SOI flip-flop designs," in 2014 IEEE International Reliability Physics Symposium, 2014, pp. SE.4.1–SE.4.7.
- [5] A. Makihara, T. Yamaguchi, H. Asai, Y. Tsuchiya, Y. Amano, M. Midorikawa, H. Shindou, S. Onoda, T. Hirao, Y. Nakajima, T. Takahashi, K. Ohnishi, and S. Kuboyama, "Optimization for SEU/SET immunity on 0.15 μm fully depleted CMOS/SOI digital logic devices," *IEEE Transactions on Nuclear Science*, vol. 53, no. 6, pp. 3422–3427, 2006.
- [6] Zongru Li, Christopher Elash, Chen Jin, Li Chen, Shi-Jie Wen, Rita Fung, Jiesi Xing, Shuting Shi, Zhi Wu Yang, and Bharat L. Bhuvu, "Efficacy of transistor stacking on flip-flop SEU performance at 22-nm FDSOI node," *IEEE Transactions on Nuclear Science*, vol. 70, no. 4, pp. 596–602, 2023.
- [7] J. Furuta, S. Sugitani, R. Nakajima and K. Kobayashi, "A Partially-redundant Flip-flip Suitable for Mitigating Single Event Upsets in a FD-SOI Process with Low Performance Overhead," 2024 IEEE International Reliability Physics Symposium (IRPS), Grapevine, TX, USA, 2024
- [8] M. Omana, D. Rossi, and C. Metra, "Novel transient fault hardened static latch," in *International Test Conference, 2003. Proceedings. ITC 2003.*, 2003, vol. 1, pp. 886–892.
- [9] Jun Furuta, Kentaro Kojima, and Kazutoshi Kobayashi, "Evaluation of heavy-ion-induced SEU cross sections of a 65-nm thin BOX FDSOI flip-flops based on stacked inverter," in 2018 18th European Conference on Radiation and Its Effects on Components and Systems (RADECS), 2018, pp. 1–6.

A preliminary study to accurate far-localisation for wireless energy transfer in electric vehicles

Stephen Hoelzel, Heiko Hepp

Faculty I – Electrical Engineering and Information, Technology

Hochschule Hannover University Applied Science and Arts

Ricklinger Stadtweg 120, 30459 Hannover, Germany

Email: Stephen.hoelzel@hs-hannover.de

Keywords : inductive wireless power transfer, localisation, positioning, Ultra Wide Band, standardisation

Abstract Electromobility is growing at different rates in different markets around the world. The charging infrastructure has to follow the increasing degree of electrification of cars. In this case, it can be considered if the normal charging with a physical connection such as a cable must be set or if the advantages of the new technology can be used to improve the charging process: inductive wireless power transfer. This technology needs a high positional accuracy between the ground coil and the vehicle. This paper will discuss different localisation technologies according to their suitability.

Introduction Electromobility is growing, although it's still developing in most markets. In those markets where the conditions are right and people accept the challenges of the new technology, electromobility can play a leading role. In Norway, registrations of battery electric cars and plug-in electric hybrids have risen to 89% - and are still rising [1]. China will increase its share of electric vehicles to over 50% by 2024 for the first time [2], [3]. Germany is already struggling and has lost its pole position in electric vehicle sales. It has been overtaken by the UK [4]. Sales in Germany have fallen to 13.5% [5] and are so low because reservations about electromobility remain stable: low-cost models, insufficient charging infrastructure and the range of EVs are not acceptable [6], [7], [8].

The technology that can revolutionise the charging of electric vehicles is inductive wireless power transfer (iWPT). The main advantage of this technology is that it provides wireless charging. The energy doesn't need a physical connection between two points because the energy is transmitted through the air by a magnetic field. This brings new challenges: good positioning between the ground coil and the car coil is necessary for the power transfer itself and also for efficient charging.

Standardization Wireless Power Transfer The standardisation process for iWPT has been greatly improved. In particular, SAE J2954 for the North American region and IEC 61980 for the European region are well known. These standards already provide guidance for 2022 and describe how to build an interoperable charging system. The unexplained positioning differences and test conditions for electromagnetic compatibility (EMC) and electromagnetic fields (EMF) are milestones. Standardisation has overcome the last hurdle and work can begin on industrial applications.

Positioning accuracy is crucial. The standard specifies positioning tolerances of 14 cm in the longitudinal direction and 20 cm in the lateral direction. These conditions also affect the cost of the coils, because the larger the working area that needs to be covered, the more expensive it becomes. Conversely, the more accurate the positioning can be, the smaller the positioning tolerances can be. That is the reason why most major manufacturers work at some form of positioning system. The "Differential Inductive Positioning System" (DIPS) can be highlighted because it was referenced in SAE J2954 at the end of 2023. This type of positioning system can be categorised as mutual induction, which is well known in the research community for near field detection. However, DIPS wants to extend its application to far-field detection so that it can realise far-field localisation between the ground coil and the car. The announcement of DIPS has not yet overcome and it still has to prove its suitability under real conditions.

Positioning There are a number of localisation technologies that differ in terms of accuracy. This aspect is crucial for iWPT. The following technologies will be discussed in more detail: Differential GPS, Bluetooth Low Energy, Wi-Fi, Camera, LiDAR and UWB. These technologies will be compared in terms of their characteristics and classified in terms of their suitability for long range localisation.

Alternative Positioning Technologies The Global Navigation Satellite System (GNSS) brings all the world's satellite systems together, including GPS (USA), Galileo (EU) and GLOSNASS (Russian Federation). The position is determined by measuring the transit time of radio signals at the receiver. The received signal contains information about the current position of the satellite. Three different satellite signals are needed to determine the 3D space for the current position. Since most receivers do not have the required accuracy, a fourth satellite signal must be used as a reference signal for evaluation. This is done by hyperbolic positioning. The accuracy of the position evaluation reaches 5 to 20 metres. The accuracy can be improved by using correction data. The so-called differential GPS (DGPS) receives its correction data from stationary reference stations. The accuracy is reduced to 0.3 to 2.5 metres.

Bluetooth Low Energy (BLE) is an evolution of the Bluetooth standard for the Internet of Things (IoT). For this reason, BLE has integrated localisation techniques. Positioning can be achieved in several ways. Typically, there are many stationary stations (called beacons) that have received the signal from the transmitter. It is possible that more than one beacon is used to evaluate the signal for localisation, but one beacon may be sufficient for positioning. BLE also uses radio waves and the level strength of the signal is evaluated. This approach is called Received Signal Strength Indicator (RSSI). Depending on the configuration and signal strength, an accuracy of up to 5 metres can be achieved. Since version 5.1, BLE has added the evaluation of the Angle of Arrival (AoA), which can be combined with RSSI to reduce significantly the accuracy.

Table 1: Overview Localisation Technologies

	DGPS	BLE	Wi-Fi	Camera	LiDAR	UWB
Range	infinity	< 100 m	< 500 m	< 20 m	< 100 m	< 200 m
Accuracy	0,3 - 2,5 m	10 - 500 cm	1 - 10 m	0,1 - 1 m	1 cm	10 - 30 cm
Scalability	high	High	high	medium	low	high
Cost	medium	low	medium	medium	high	medium
Data Rate	none	low	high	/	/	medium
Reliability	medium	low	low	medium	medium	high
Power	medium	low	medium	medium	high	low
Latency	< 100 ms	< 5 s	< 5 s	< 100 ms	< 100 ms	< 1 ms

Another localisation technology that also uses radio waves is Wireless Fidelity (Wi-Fi). This technology is easy to integrate because of the existing infrastructure. The most common approach is RSSI as BLE, where the signal strength is used to evaluate the position via a multilateration algorithm. This requires multiple access points on the infrastructure side. In addition, Wi-Fi offers the possibility to evaluate the transmission time. This approach is called Time of Flight (ToF) and achieves a higher accuracy. This approach has been implemented since Wi-Fi version 6 as Round-Trip-Time (RTT) and required a high standard of hardware due to the fast transmission time evaluation. Much of the hardware in use doesn't support this new standard today.

In addition to technologies based on the receiver-transmitter principle, localisation can also be achieved through external features evaluated by camera-based systems. The environment of interest is mapped into a digital 3D localisation map. If a track is driven, localisation can be achieved by identifying features around the track. The detection of the features, which depends on whether conditions exist, determines the achievable accuracy. The accuracy can reach values from 0.1 to 1 metre, which is a great effort because of the mapping.

Localisation can be achieved by concentrating light like a laser. One approach currently being explored is Light Detection and Ranging (LiDAR). The environment is continuously scanned by the laser and compared with the recorded features. This only works when mapping is complete. Compared to a light-based approach, a laser achieves significantly

better accuracy in the centimetre range.

Table 1 summarises all the localisation technologies presented. Based on this summary, it should be decided which localisation technology is most suitable for iWPT. There are real-time requirements for location while driving that can't be met by BLE and Wi-Fi. In addition, ranges of more than 100 metres must be reliably achieved, which is the case for all technologies. The most important specification is accuracy, as iWPT's requirements are tough and positioning has to succeed in a 14 cm x 20 cm window. This requires high accuracy of less than 10 cm, which only LiDAR and UWB can provide. The high overall cost of LiDAR doesn't make it scalable for a high volume market, leaving only UWB as the most suitable far-field localisation technology for iWPT.

Ultra Wide Band The general description of the transfer behaviour of electromagnetic signals describes in the telecommunications technology Friis transmission equation (see formula (1)). Friis' explained the transfer behaviour between transmitter and receiver in a free space. Besides the transmitting power P_t and the gain power of the antenna for transmitter G_t and receiver G_r is described by the propagation of the signal in free space and its continuous decrease through isotropic propagation. That can be determined by the wavelength λ and range d as sphere. The result is the signal strength P_r .

$$P_r = P_t + G_t + G_r + 20 \log \left(\frac{\lambda}{4\pi d} \right) \tag{1}$$

It is important to note that this formula is a very simplified model and does not take into account most real world effects such as signal attenuation due to obstructions and reflections from the ground or buildings. Nevertheless, this formula approximates the transmitter signal strength as a function of the signal wavelength and the distance.

One of the most important effects are ground reflections. The work [9] adapted the last term (see formula (2)), which describes the decrease in signal strength due to isotropic propagation.

$$P_r = P_t + G_t + G_r + 10 \cdot \log \left(\frac{16\pi^2 \cdot f_b \cdot f_L \cdot f_H \cdot d'^2 \cdot d''^2}{c^2 [f_b \cdot (d''^2 + \Gamma^2 \cdot d'^2) + 2\Gamma \cdot d' \cdot d'' \cdot I]} \right) \tag{2}$$

Ground reflections show the influence of Fresnel zones. Fresnel zones describe a channel around the line-of-sight (LOS) connection between the transmitter and receiver. If there are any obstacles in this channel, the signal strength will be attenuated. The signal behaviour looks like jumping (see Figure 1) because the disturbed part can impact as increase

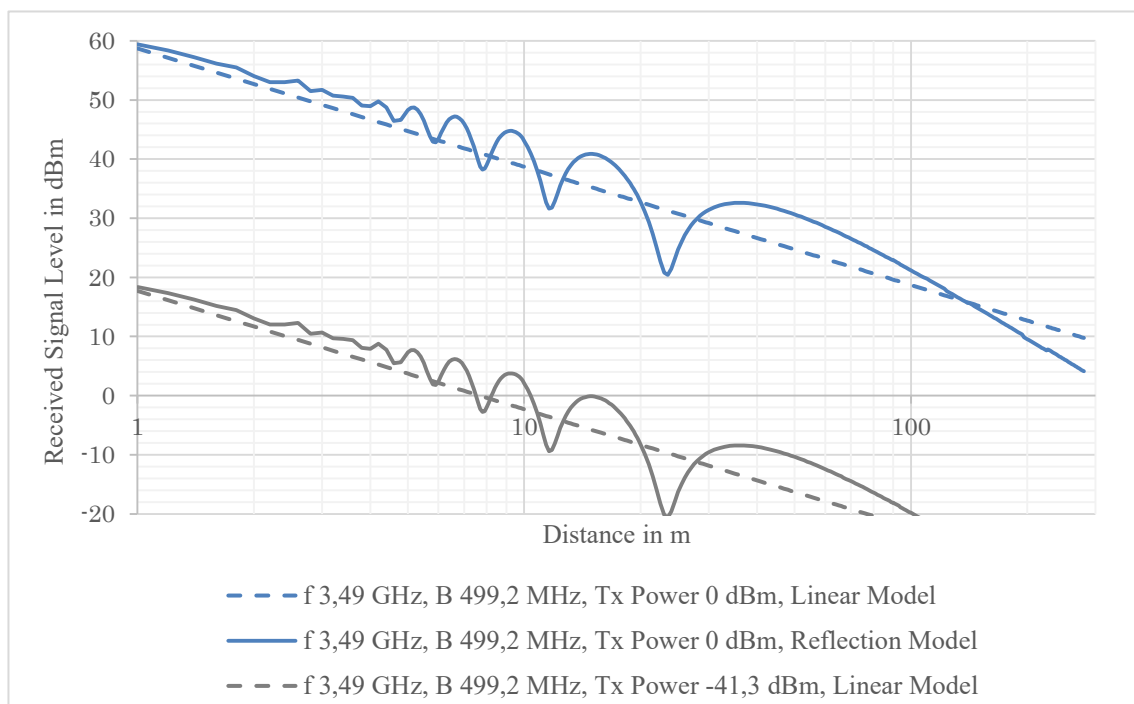


Figure 1: Friis' transmission equation with/without ground reflection

or decrease which depends on the arrival of the signal.

In addition to these interference effects, the transmit power has a significant impact on the achievable distance. Due to the signal characteristics, UWB can operate with low transmit power, which is why the peak power of UWB is -41.3 dBm/MHz. However, this limit can be exceeded if the application is permitted or the number of transmissions per minute is not too high. The achievable distance increases from about 10 metres to about 300 metres.

Future Work The most important specifications, range and accuracy, will be investigated under real conditions. Initially, effects such as signal damping and obstacle reflections should be determined theoretically in simple experimental setups. The transferability to urban areas will be determined and some countermeasures will be developed if necessary. Another point of investigation is to set up a UWB network to investigate some differential approaches such as TDoA or ToF. The aim is to prove that these approaches are suitable for urban areas. Different evaluation boards from two well-known chip manufacturers will be test under real conditions.

References

- [1] „Verteilung der Antriebsarten bei Pkw-Neuzulassungen in Norwegen in den Jahren 2015 bis 2024“, Statista. Accessed: 7. Februar 2025. [Online].
- [2] „Absatz von Personenkraftwagen mit alternativem Antrieb in China von Januar 2022 bis Dezember 2024“, Statista. Accessed: 7. Februar 2025. [Online].
- [3] „Absatz von Personenkraftwagen in China von Januar 2022 bis Dezember 2024“, Statista. Accessed: 7. Februar 2025. [Online].
- [4] T. Wicke, „Elektroauto-Verkäufe 2024: Chinesische Hersteller auf dem Vormarsch, Stagnation in Europa“, Fraunhofer-Institut für System- und Innovationsforschung ISI. Accessed: 7. Februar 2025. [Online].
- [5] „Anzahl der Neuzulassungen von Elektroautos in Deutschland von 2003 bis Januar 2025“, Statista. Accessed: 7. Februar 2025. [Online].
- [6] „Mobilitätsmonitor 2022“, Deutsche Akademie der Technikwissenschaften, Feb. 2023.
- [7] „DAT Report 2024“, Deutsche Automobil Treuhand GmbH, Feb. 2024.
- [8] „Mobilitätsmonitor 2024“, Deutsche Akademie der Technikwissenschaften, Apr. 2024.
- [9] P. Supanakoon, S. Kaewsirisin, S. Promwong, S. Noppanakepong, und J. Takada, „Ground Reflection Path Loss Based on Average Power Loss for Ultra Wideband Communications“, in 2007 Asia-Pacific Microwave Conference, Dez. 2007, S. 1–4. doi: 10.1109/APMC.2007.4554832.

Respirometer by a piezo device and its application to triage

Tomoya YOSHIDA*

* Faculty of Computer Science and Systems Engineering, Okayama Prefectural University
111 Kuboki, Soja, Okayama 719-1197, Japan
E-mail: tyoshida@oka-pu.ac.jp

Keywords: piezo device, triage, Respirometer

Among the variety of possible applications of piezo devices to health care, we chose to focus on triage. We found that blowing on the piezo device generated several hundred millivolt voltage and also it synchronizes with the respiration. Our detail investigations on the phenomena showed that it was caused by the pyroelectric effect. In general, the piezo device when used as a sensing device generates output voltage in a battery-less manner and also functions as a buzzer, which can lead to a compact, simple and low-power respirometer. Here the piezo device was used as a base of respirometer, and used not only as a respirometer but also as an alarm sound generator. Thus the proposed respirometer was realized only by one piezo device and a low-powered microprocessor driven by a small battery. We applied the respirometer to triage and realized a triage sensing system. In the system, we employed the triage priority determination procedure defined as an international standard. The triage sensing system set in a mask detects respiration and displays its condition by turning an LED on and off synchronizing the respiration and also generates the alarm sound when the respiration falls into the pre-specified ill-conditions. Figure 1 shows a device for triage sensor. Figure 2 shows the measurement principles used to detect the respiration using a piezo device. The exhaled hot air arrives at the surface of the piezo device when the patient breathes, and a temperature difference $\Delta T(t)$ occurs between the mouth side and other side of the device. Then the device generates a voltage $E_r(t)$ in accordance with the transfer function of voltage with respect to temperature. Figure 3 shows the LED lighting in synchronizing with the respiration.

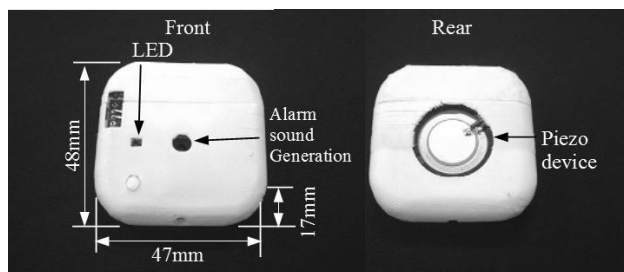


Fig. 1 The developed triage sensor

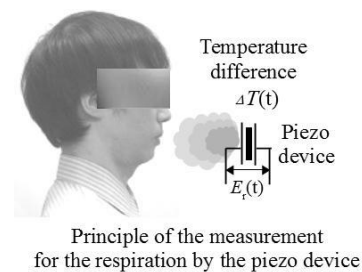


Fig. 2 Measurement principles of respiration using a piezo

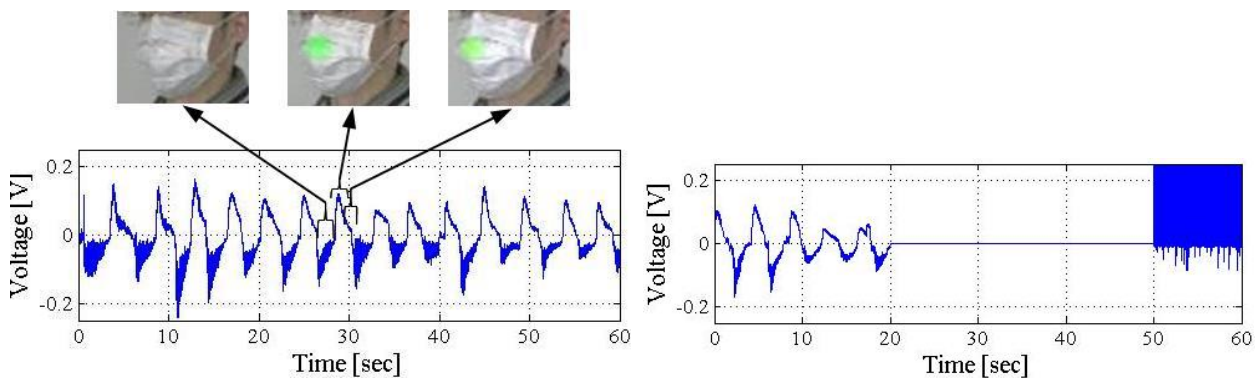


Fig. 3 Respiration signals by the sensor function and the sound waves by the actuator function of one piezo device

References

Yoshida T, Kobayashi K, Kurihara Y, Shiroi N, Watanabe K, Multiple-input/multiple-output characteristics of piezo devices and an application for triage. *IEEE Sens J*17(5), 2017, pp.1434–1442. (references)

Using deep learning for plant root point detection in agricultural robotics

Frank STOLLMEIER, Liu WANGCHU, Hanno HOMANN

Faculty I – Electrical Engineering and Information, Technology

Hochschule Hannover University Applied Science and Arts

Ricklinger Stadtweg 120, 30459 Hannover, Germany

Email: frank.stollmeier@hs-hannover.de

Keywords : Precision farming, Agricultural robotics, Weeding, Deep learning, Object detection

Abstract

The use of synthetic herbicides for weed control is prohibited in organic farming, but existing alternative methods are often less effective. In some crops, especially vegetables, weeds must be removed manually, which is time-consuming and costly. To address this issue, we are developing a weeding robot that employs image-based AI to identify individual plants and uses a mechanical tool to remove the weeds. This study compares two deep learning models, YOLOv8 and FCOS, for detecting the plant root points. Our results demonstrate that FCOS detects the root points with a higher precision than YOLOv8, but at the cost of a slower inference.

Introduction

The use of herbicides for weed control can pose a risk to human health and harm the environment. Additionally, weeds are increasingly developing resistance to herbicides. In order to avoid these negative effects, herbicides are not used in organic farming. However, the existing methods for organic weed control are less effective or very time-consuming. To address these issues, we are developing an automated system for mechanical weed control in vegetable cultivation. The system detects each plant and classifies it as weed or crop using artificial neural networks. The weeds are removed using a precise mechanical weeding tool. The motivation of this development is to reduce costs and risks in organic weed control, thereby supporting the transition from conventional to organic farming and facilitate the regional cultivation of organic vegetables despite high labor costs.

In order to remove individual plants, the robot system requires a fast, accurate and robust visual detection of the plants. Specifically, we need to detect the location of the root point of each plant. The root point is defined as the point where the stem of a plant meets the ground surface. This task presents two challenges: First, the plants have a very high variability in their appearance, depending on the species, their age, their health and the availability of water and nutrients. Second, the stem is often obscured by leaves, which can be the leaves of the same plant or leaves of other plants.

Commonly used deep learning models for keypoint detection are Keypoint RCNN [1], PoseTED (based on YOLOv4) [2], or CenterNet [3]. A typical use case for these models is human pose estimation, where the keypoints are shoulders, elbows, knees, feet or hands. In simple cases, we could use such a keypoint detection model to find the root points. However, some plants, like grass for example, often grow in dense clusters. In these cases, it makes more sense to annotate the area of the cluster instead of every single stem. Also when the exact position of the root point is not visible, it is preferable to annotate the area that contains the root point instead of a point at a possibly incorrect position. For these reasons, we investigate the use of object detectors instead of keypoint detectors to predict the root points. The two object detection models that we compare in this study are YOLOv8 [4] and FCOS [5].

Materials and Methods

The images were recorded on different fields for the organic cultivation of onions in Lower Saxony, Germany, at several days between 1 and 10 weeks after sowing and at several locations on the field to include the temporal and spatial variability of the field in the dataset. The images were recorded with an RGB camera with a resolution of 2048 x 1536, which is mounted on a data recording platform specifically designed for collecting images of plants on a field. In order

to ensure controlled light conditions, the recording platform is equipped with an LED light and a casing that protects the inside from surrounding light.

The root points that can be precisely located were annotated as points. The root point clusters or uncertain positions of root points were annotated as bounding boxes. In total, our dataset consists of 1285 annotated images, including 9737 onions and 4263 weeds.

During the preprocessing of the training, we convert each point label to a small bounding box of a fixed size with its center at the position of the point. This way we can train object detectors as if it was a normal object detection task. Both models, FCOS and YOLOv8, were trained on the same dataset using the Adam optimizer with a learning rate of 0.001. We used a standard laptop with an Nvidia GeForce RTX 3060 and stopped the training of both models after 3 hours.

Results

The quality of the two models was evaluated based on the average precision calculated at an intersection over union threshold of 0.50. The results are summarized in Table 1. An example image with the predictions is shown in Figure 1.

Model	AP50 (onions)	AP50 (weeds)	Inference time [ms]
YOLOv8	0.969	0.871	39
FCOS	0.967	0.924	638

Table 1 Average precision after training both models on the same dataset and for the same duration.

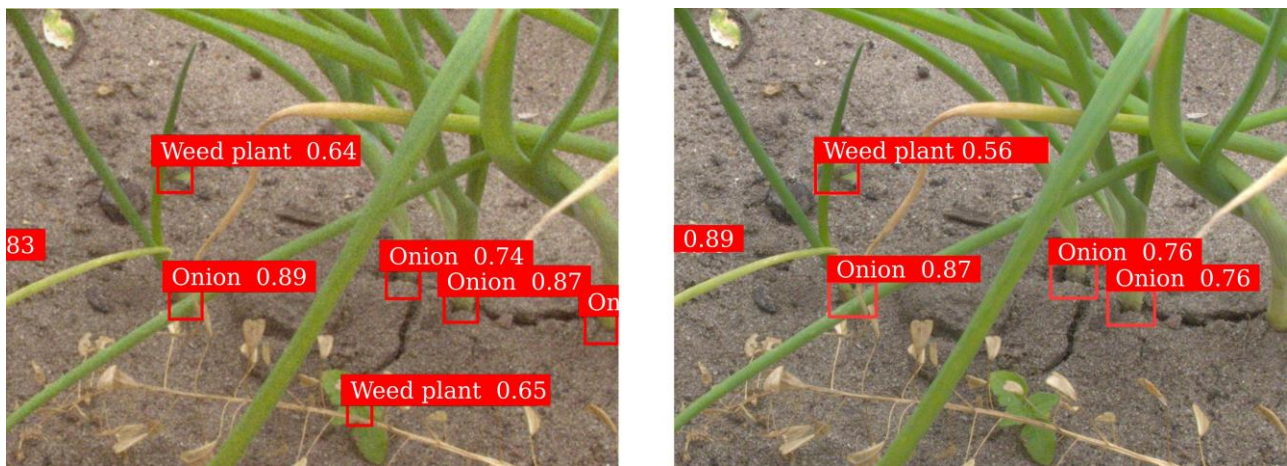


Figure 1 Example image from the validation dataset with the predictions of FCOS (left) and YOLOv8 (right).

Discussion

The results show that both FCOS and YOLOv8 detect the onion root points with a high precision. The precision for weed root points is smaller in both models. This is not surprising as the number of weeds in our dataset is smaller than the number of onions. Secondly, the weeds are more diverse because the category "onion" contains plants of exactly one species while the category "weeds" contains all other species on the field. FCOS seems to cope better with this difficulty than YOLOv8. However, the higher precision of the FCOS predictions comes at the cost of a much slower inference compared to YOLOv8.

In subsequent studies, we plan to test additional models and investigate techniques to improve the robustness of root point detection under challenging conditions.

Acknowledgement

This research was funded by the German Federal Ministry of Education and Research (BMBF), grant number 03FHP226.

References

- [1] K. He, G. Gkioxari, P. Dollár and R. Girshick, "Mask R-CNN", 2017 IEEE International Conference on Computer Vision (ICCV), Venice, Italy, 2017, pp. 2980-2988, doi: 10.1109/ICCV.2017.322.
- [2] A. Jeny, M. Junayed, and M. Islam. 2021. "PoseTED: A Novel Regression-Based Technique for Recognizing Multiple Pose Instances", In *Advances in Visual Computing: 16th International Symposium, ISVC 2021, Virtual Event, October 4-6, 2021, Proceedings, Part I*. Springer-Verlag, Berlin, Heidelberg, 573–585. doi: 10.1007/978-3-030-90439-5_45.
- [3] K. Duan, S. Bai, L. Xie, H. Qi, Q. Huang and Q. Tian, "CenterNet: Keypoint Triplets for Object Detection", 2019 IEEE/CVF International Conference on Computer Vision (ICCV), Seoul, Korea (South), 2019, pp. 6568-6577, doi: 10.1109/ICCV.2019.00667.
- [4] R. Varghese and Sambath M., "YOLOv8: A Novel Object Detection Algorithm with Enhanced Performance and Robustness", 2024 International Conference on Advances in Data Engineering and Intelligent Computing Systems (ADICS), Chennai, India, 2024, pp. 1-6, doi: 10.1109/ADICS58448.2024.10533619.
- [5] Z. Tian, C. Shen, H. Chen and T. He, "FCOS: Fully Convolutional One-Stage Object Detection", 2019 IEEE/CVF International Conference on Computer Vision (ICCV), doi: 10.1109/ICCV.2019.00972.

Bonding of CFRTP and SPCC Using Porous Plating and Evaluation of Strength by Single-Lap Shear Test

Manato KANESAKI*, Kazuki TSUJIKAWA**, Tadao FUKUTA and Koichi OZAKI**

* Faculty of Computer Science and Systems Engineering, Okayama Prefectural University

111 Kuboki, Soja, Okayama 719-1197, Japan

E-mail: Manato_k@cse.oka-pu.ac.jp

**Graduate School of Computer Science and System Engineering, Okayama Prefectural University

111 Kuboki, Soja, Okayama 719-1197, Japan

Keywords: CFRTP, Porous Plating, Dissimilar material joining

In the automotive and aerospace industries, the development of joining methods for dissimilar materials is crucial for the optimal application of metallic materials and carbon fiber reinforced plastics (CFRP). To enhance the bonding strength between these materials, we focused on porous nickel plating. The porous nickel plating used in this study consists of a porous nickel-based plating formed on cold-rolled steel plate (SPCC). Fukuda et al. [1] have reported that this porous nickel plating improves the bonding strength between metals and plastics. This result suggests that direct bonding between CFRP and SPCC with porous nickel plating is feasible.

This study aimed to determine the optimal plating thickness that maximizes the bonding strength between SPCC and CFRP while preventing delamination between the SPCC and the plating layer. Additionally, to mitigate galvanic corrosion, oxidized specimens with the identified optimal plating thickness were prepared, and the effect of oxidation treatment on bonding strength was evaluated. Here, in this study, laminates using carbon fiber and polyamide 6 (CF/PA6) was prepared as the CFRP. In addition, the specimen shape and dimensions shown in Fig. 1 were based on the study by Tanabe et al. [2]

It was found that for SPCC coated with nickel plating ranging from 20 μm to 40 μm in thickness, the shear strength increased with increasing plating thickness (Table 1). Subsequently, oxidation treatment was applied to SPCC with a 40 μm plating thickness, which exhibited the highest bonding strength with CF/PA6, and shear tests were conducted again. The results demonstrated that oxidation treatment further improved the shear strength.

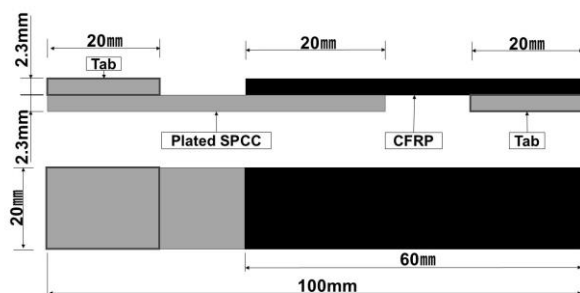


Fig. 1 Schematic diagram of single lap shear test specimen

Table 1 Average of shear strength and standard deviation between Plated SPCC and CF/PA6 laminates.

Specimen name	Average of shear strength [MPa]	S.D.[MPa]
20 μm Plated SPCC	8.64	1.08
30 μm Plated SPCC	9.66	3.10
40 μm Plated SPCC	14.7	1.24
40 μm Plated SPCC + Oxidized	19.0	0.83

References

- [1] C. Fukuda, K. Takahashi, Y. Nishimura, and K. Ozaki, "Porous Nickel Plating as a Surface Treatment for Bonding Dissimilar Materials", *Adv. Experi. Mech.*, Vol. 6, pp. 65-70, Dec. 2021.
- [2] D. Tanabe, T. Horiuchi, and K. Nishiyabu, "Effects of Thickness of Plymer Based Energy Director on Ultrasonic Spot Welding Behavior of Woven-CF/PPS Laminates", *J. Soc. Mater. Sci. Jpn.*, Vol. 69, No.5, pp.373-378, May 2020.

AI Light Room – Intelligent Lighting for Unconscious Patients in Anesthesia and Intensive Care

Mike OTTO, Jens Christian WILL, Yavuz KÖCER

Faculty I – Electrical Engineering and Information, Technology

Hochschule Hannover University Applied Science and Arts

Ricklinger Stadtweg 120, 30459 Hannover, Germany

Email: mike.otto@hs-hannover.de

Keywords: Light Therapy, Computer Vision, AI, Healthcare

1. Introduction

Over the past 18 years, the total number of surgeries performed annually has risen by 52%, reaching nearly 15 million in 2023 [2]. On average, 40,000 patients undergo anesthesia every day in Germany [1]. This growing volume underscores the importance of reducing postoperative recovery times. Faster recovery benefits not only the patients, by improving their quality of care, but also enhances the efficiency of the healthcare system and lowers associated costs.

A pilot study by Taguchi et al. [7] examined bright light therapy in postoperative patients, focusing on delirium prevention and circadian rhythm regulation. Eleven esophageal cancer patients were randomized into an intervention group (5000-lux light therapy) or a control group (natural light). Results revealed that the intervention group had significantly lower delirium scores on the third day of light therapy and began mobilization approximately two days earlier than the control group. Joseph [6] reviewed the effects of both natural daylight and artificial light on health outcomes in healthcare settings. Light influences human health and performance by regulating the circadian system, affecting mood and perception, and supporting essential chemical reactions in the body. Proper regulation of the circadian system through light exposure has been shown to reduce hospital stays, alleviate depression, improve sleep patterns, mitigate agitation in dementia patients, and relieve pain. Joseph's findings highlight the importance of incorporating light sources that closely mimic the natural spectrum of sunlight in healthcare environments.

A meta-analysis by [4] evaluated the role of light therapy in improving sleep, depression, neuropsychiatric behaviors, and cognition in individuals with dementia. Pathologies affecting the suprachiasmatic nucleus, the body's "internal clock," disrupt circadian rhythms critical for sleep, emotional regulation, and cognitive functions. The synchronization of these rhythms depends heavily on light exposure. The analysis suggests that light therapy can serve as a supportive intervention for improving these outcomes in dementia patients.

In summary, existing research demonstrates the significant benefits of light exposure on human health, particularly in enhancing sleep quality, mood, and recovery times. These findings have also contributed to shorter hospital stays. Recent advancements in LED technology allow for light spectra that more closely resemble natural daylight, underscoring the need for innovative devices capable of fully utilizing this spectrum. However, no studies to date have examined light intensities exceeding 10,000 lux, despite midday sunlight reaching up to 100,000 lux. Additionally, there is a lack of research linking light exposure to vital parameters with analyses supported by artificial intelligence.

2. Project Goals

This project aims to develop and test an AI-powered lighting system using high-power LEDs to generate illumination levels close to natural sunlight, reducing stress and promoting healing in unconscious patients during anesthesia and intensive care.

Beyond immediate improvements in patient care, the project fosters new research in medical light therapy and AI-assisted diagnostics. The societal impact is significant, contributing to improved patient safety and quality of life during and after surgical procedures by reducing stress and optimizing the healing process.

By the project's completion, the foundation for clinical integration will be established, including a functional, tested

demonstrator, validated efficacy and safety, workflow integration, and training materials for medical personnel.

3. Approach

3.1 Hardware

For the first prototype, we utilize two COB ("Chip-on-Board") LEDs emitting white light, along with three high-power LEDs emitting red, green, and blue light.

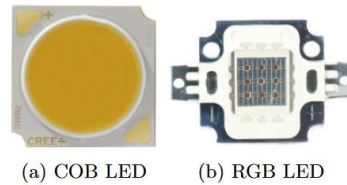


Figure 1: LED types used in the prototype.

COB LEDs integrate multiple LED chips onto a thermally efficient substrate, enabling high packing density and increased luminous output within a compact module. A uniform phosphor coating ensures consistent light quality and color temperature [3]. These LEDs provide a bright, uniform illumination, making them well-suited for our application. The combination of COB and RGB LEDs allows flexible adjustment of light color and temperature. Pulse-Width Modulation (PWM) is employed for dimming control.

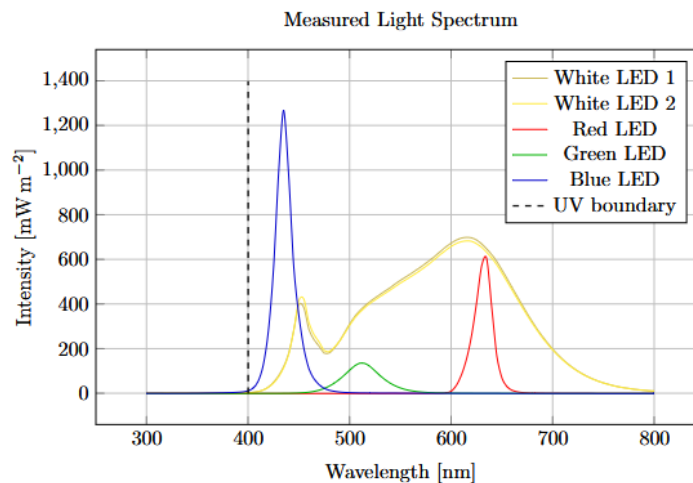


Figure 2: Measured Light Spectrum

The above plot illustrates the spectral distribution of emitted light intensity as a function of wavelength for each of the five LEDs used. As observed, the combination of different LED types enables reproduction of the entire visible spectrum while ensuring that no hazardous ultraviolet (UV) radiation is emitted.

At a distance of 10 cm from the patient's face—our target application distance—a single COB LED achieves a peak brightness of 60,000 lx. This allows us to simulate sunlight exposure, facilitating research into its potential effects on patient recovery. With a maximum brightness of 4,000 lx, the RGB LEDs are significantly dimmer than the COB LEDs but still sufficiently bright for their intended purpose of generating light with adjustable color and temperature.

However, the high power of these LEDs presents a significant thermal challenge. Without adequate cooling, COB LEDs generate enough heat to melt the soldering material, effectively desoldering themselves. To mitigate this issue, the LEDs are mounted onto a heat sink with an active cooling fan, ensuring efficient heat dissipation and maintaining stable operation.

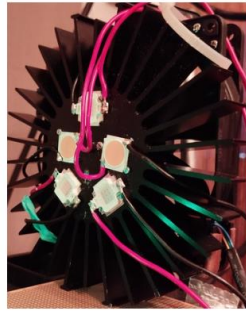


Figure 3: Cooling Block with LEDs

The control system for light application is implemented using a Raspberry Pi 5. Its affordability, extensive library support, and compatibility with a wide range of peripherals make it an ideal choice for early prototyping of our device.

3.2 Eye State Recognition

In our use case, patients' eyes are expected to remain closed; however, due to high brightness levels, protective measures are necessary. To prevent unintended exposure, we integrate a Convolutional Neural Network (CNN) with a camera to monitor the patient's eye state (open vs. closed) in real-time. If an open eye is detected, the system promptly reduces the LED brightness or shuts off the LEDs entirely.

Given the limited computational resources of the Raspberry Pi and the requirement for rapid response times, we designed a custom CNN with approximately 270,000 parameters. This corresponds to just 5.4% of the size of MobileNetV3, one of the most widely used CNNs for mobile and low-power devices [5].

Our model achieved inference times below 18 ms when benchmarked on the Raspberry Pi 5 (without utilizing AI accelerators). Despite its significantly smaller size and improved inference speed, the model maintained accuracy above 99% on the MRL-Eye dataset, a standard benchmark for eye state detection. Detailed results and elaborations on this custom-designed CNN and the associated algorithm will be published in the future.

4. Outlook

The next step towards developing a market-ready product involves integrating the LEDs, their corresponding electronic control circuits, and the camera into a fully functional prototype. The design of this prototype is currently in progress and will be published once finalized.

The following image illustrates an earlier prototype, which, despite demonstrating core functionality, was ultimately deemed too large for its intended application.



Figure 4: Previous Prototype Design

Once completed, the functional prototype will undergo extensive clinical trials to investigate the potential benefits of controlled, artificial light application in improving key health metrics for patients in intensive care. By precisely modulating light exposure, we aim to explore its effects on circadian rhythm regulation, sleep quality, and overall patient recovery.

In parallel, we are evaluating the feasibility of utilizing hardware optimized for AI applications, such as the NVIDIA Jetson series. This integration could significantly enhance processing capabilities, allowing for faster and more accurate

eye-state detection. Moreover, leveraging AI for real-time analysis of patient health data could unlock additional functionalities, such as automated monitoring and predictive analytics, thereby broadening the range of possible applications for the final product.

Beyond computational efficiency, embedding AI-powered processing could also facilitate adaptive light modulation based on individual patient responses, further personalizing the treatment approach. As we refine the prototype, we will continue exploring cutting-edge hardware and AI-driven solutions to maximize both its effectiveness and usability in clinical environments.

References

- [1] Moderne Narkose wird 175 Jahre alt. <https://www.dgai.de/aktuelles-patientinnen-projekte/pressemitteilungen/66-pressearchiv-2021/933-moderne-narkose-wird-175-jahre-alt.html>.
- [2] Operationen und Prozeduren der vollstationären Patientinnen und Patienten in Krankenhäusern. https://www.gbe-bund.de/gbe/pkg_olap_tables.prc_set_hierlevel?p_uid=gast&p_aid=3616918&p_sprache=D&p_help=2&p_indnr=662&p_ansnr=29398852&p_version=4&p_dim=D.390&p_dw=43173&p_direction=drill
- [3] Understanding CoB LEDs. <https://lumileds.com/technology/led-technology/understanding-cob-leds/>
- [4] Aini et al. The Effects of Light Therapy on Sleep, Depression, Neuropsychiatric Behaviors, and Cognition Among People Living With Dementia: A Meta-Analysis of Randomized Controlled Trials. *The American Journal of Geriatric Psychiatry: Official Journal of the American Association for Geriatric Psychiatry*, 32(6):681–706, June 2024.
- [5] Howard et al. Searching for MobileNetV3, November 2019.
- [6] Anjali Joseph. The Impact of Light on Outcomes in Healthcare Settings.
- [7] Toyoe Taguchi, Masahiko Yano, and Yoshihiro Kido. Influence of bright light therapy on postoperative patients: A pilot study. *Intensive and Critical Care Nursing*, 23(5):289–297, October 2007.

Agenda

PROGRAM	10:00-10:15	Opening Welcome Message: Chaired by Prof. Takashi OYAMA (Okayama Prefectural University) /Prof. Yutaka ISHII (Okayama Prefectural University) /Prof. Franz KALLAGE (Hanover University of Applied Sciences and Arts)	Room 8105
	10:15-10:20	Group Photo Session: Chaired by Prof. Takashi OYAMA (Okayama Prefectural University)	
	10:30-12:00	VR session : Organized by Prof.Yutaka ISHII (Okayama Prefectural University) Poster session : Organized by Prof. Franz KALLAGE (Hanover University of Applied Sciences and Arts)	
	101 (VR demo)	VR Devices for Communication Enhancement via Virtual Characters /Yutaka ISHII (Okayama Prefectural University) & Lab	
	102	Engineering a Tablet Filling System with CODESYS 3.5 /Jasper DEHMEL (Hanover University of Applied Sciences and Arts)	
	103 (VR demo)	VR and Haptic Devices for Health and Medical Care /Masanao KOEDA (Okayama Prefectural University) & Lab	
	104	CFD Based Simulation and Optimization of a Rotary Chamber Machine /Christoph SCHMITT (Hanover University of Applied Sciences and Arts)	
	105	Motion capture experience using mocopi /Shunsuke OTA (Okayama Prefectural University) & Lab	
	12:00-13:00	Lunch Break	
	13:00-13:10	Opening: Welcome Message & Sakura Science Club Certificate : Chaired by Prof. Teruaki ITO (Okayama Prefectural University) /Prof. Akio GOFUKU (Okayama Prefectural University)	
	13:10-13:20	Group Photo Session: Chaired by Prof. Takashi OYAMA (Okayama Prefectural University)	
	13:20-14:20	Keynote Speech : Chaired by Prof. Teruaki ITO (Okayama Prefectural University)	
	201	Future Society by Integration of VR and AI Technologies /Tetsuro OGI (Keio University)	
	14:20-14:30	Short Break	
	14:30-15:30	Session 2 : Chaired by Prof. Naoto HARUKI (Okayama Prefectural University)	
	301	A Storage Circuit Design for Suppressing Radiation-induced Errors in FD-SOI Processes /Jun FURUTA (Okayama Prefectural University)	
	302	A Preliminary Study to Precise Far Localisation for Wireless Energy Transfer in Electric Vehicles /Stephen Detlef HOELZEL (Hanover University of Applied Sciences and Arts)	
	303	Respirometer by a piezo device and its application to triage /Tomoya YOSHIDA (Okayama Prefectural University)	
	15:30-15:40	Short Break	
15:40-16:40	Session 3 : Chaired by Prof. Akira TSUMAYA (Okayama Prefectural University)		
401	Using Deep Learning for Plant Root Point Detection in Agricultural Robotics /Frank STOLLMEIER (Hanover University of Applied Sciences and Arts)		
402	Bonding of CFRTP and SPCC Using Porous Plating and Evaluation of Strength by Single-Lap Shear Test /Manato KANESAKI (Okayama Prefectural University)		
403	AI Light Room Intelligent Lighting for Unconscious Patients in Anesthesia and Intensive Care /Mike OTTO (Hanover University of Applied Sciences and Arts)		
16:40-16:50	Closing Message: Chaired by Prof. Akira TSUMAYA (Okayama Prefectural University) /Prof. Franz KALLAGE (Hanover University of Applied Sciences and Arts) /Prof. Teruaki ITO (Okayama Prefectural University)		

<https://www.ki.ss.oka-pu.ac.jp/ohjg2025/>

Host: Okayama Prefectural University (For contact, OHJG-2025@ad.oka-pu.ac.jp)
Organizer: Okayama Prefectural University, Japan / Hanover University of Applied Sciences and Arts, Germany
Sponsor: Sakura Science Program by Japan Science and Technology Agency (JST)